Computational Aeroacoustics

for

Low Mach Number Flows (I)

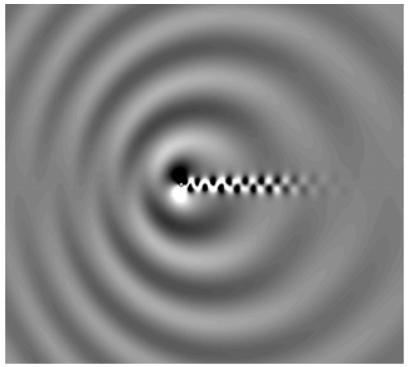

Young J. Moon

Korea University
Department of Mechanical Engineering
Seoul, Korea

Contents

I. Perturbed Compressible Equations (*PCE*) – $M \ll 1$

DNS – cylinder dipole tone (laminar)

$$\Delta p' = p - \bar{p}$$

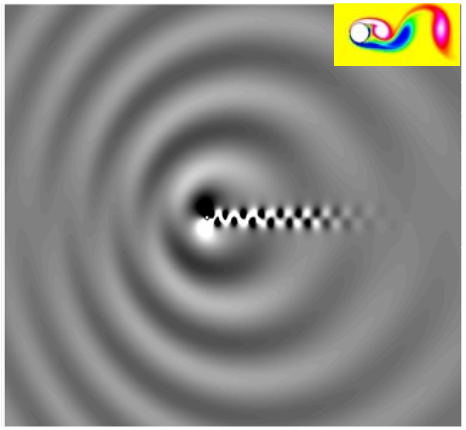

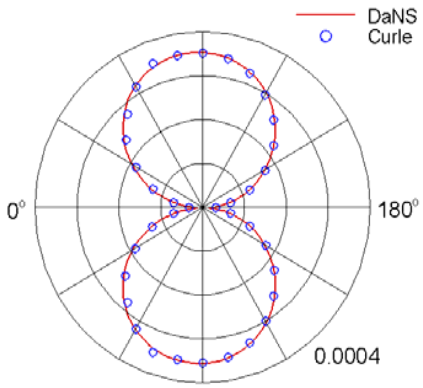

- **DNS (compressible NS)**
- **6th-order compact scheme**
  4th-order RK
- **Non-reflecting BC**
  (ETA, *Energy Transfer & Annihilating)*)

Re_D = 200, M_∞ = 0.3 @ *r = 60D*

- $\lambda_a / \lambda_h \sim 1/M_\infty$
- Large disparity between flow and acoustic scales.
- DNS becomes very costly.

CFD / CAA Hybrid method

- Hydrodynamic-Acoustic splitting concept
  - ***Hardin* & *Pope* (*1992, 1995*)**
  - ***Shen* & *Sorenson* (*1999, 2001*)**
  - ***Slimon et al.* (*1999, 2000*)**

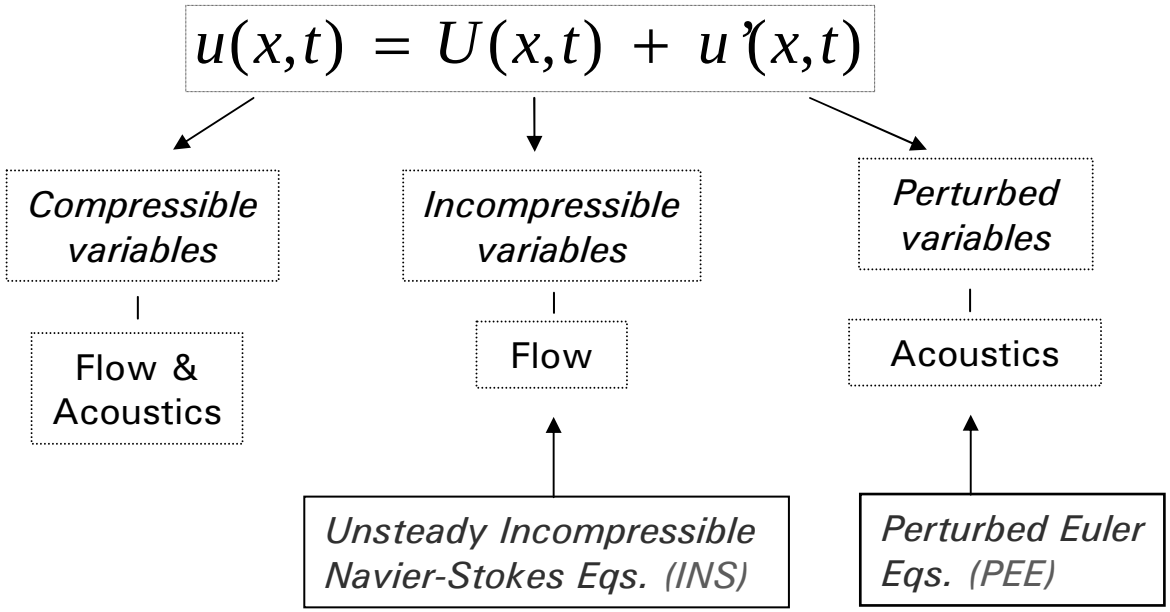

Perturbed Euler Eqs. (*PEE*)

$$\rho = \rho_o + \rho_1 + \rho', \qquad u = U + u', \qquad p = P + p'$$

$$CNS - INS = PEE$$

neglecting the viscous terms

- $$\frac{\partial \rho'}{\partial t} + \frac{\partial}{\partial x_i}(\rho u_i' + \rho' U_i) = -\frac{\partial \rho_1}{\partial t} - U_i \frac{\partial \rho_1}{\partial x_i}$$
- $$\frac{\partial}{\partial t}(\rho u'_i + \rho' U_i) + \frac{\partial}{\partial x_j}\left[u_i(\rho u'_i + \rho' U_i) + (\rho_0 + \rho_1) U_i u'_j + p' \delta_{ij}\right] = -\frac{\partial(\rho_1 U_i)}{\partial t} - U_j \frac{\partial(\rho_1 U_i)}{\partial x_j}$$

Shen & Sorenson (1999)	*Slimon et al. (2000)*
$\rho_1 = 0$	$\frac{D\rho_1}{Dt} = \frac{1}{a^2}\frac{DP}{Dt}$
$\frac{\partial p'}{\partial t} - a^2 \frac{\partial \rho'}{\partial t} = -\frac{\partial P}{\partial t}$	$\frac{Dp'}{Dt} - a^2 \frac{D\rho'}{Dt} = a^2\left(\frac{\gamma - 1}{2}\right)\frac{D\rho_1}{Dt}$

- **Slip condition at the wall**

Validation – *INS* + *PEE*

$$\Delta p' = p - \bar{p}$$

- *INS*: iterative fractional step method, 6th order for Mom. eq., 2nd order for Poisson eq., RK-3.
- Same grid for hydro & acoustic calcs. for excluding any interpolation errors.

DNS *Shen & Sorenson (PEE)*

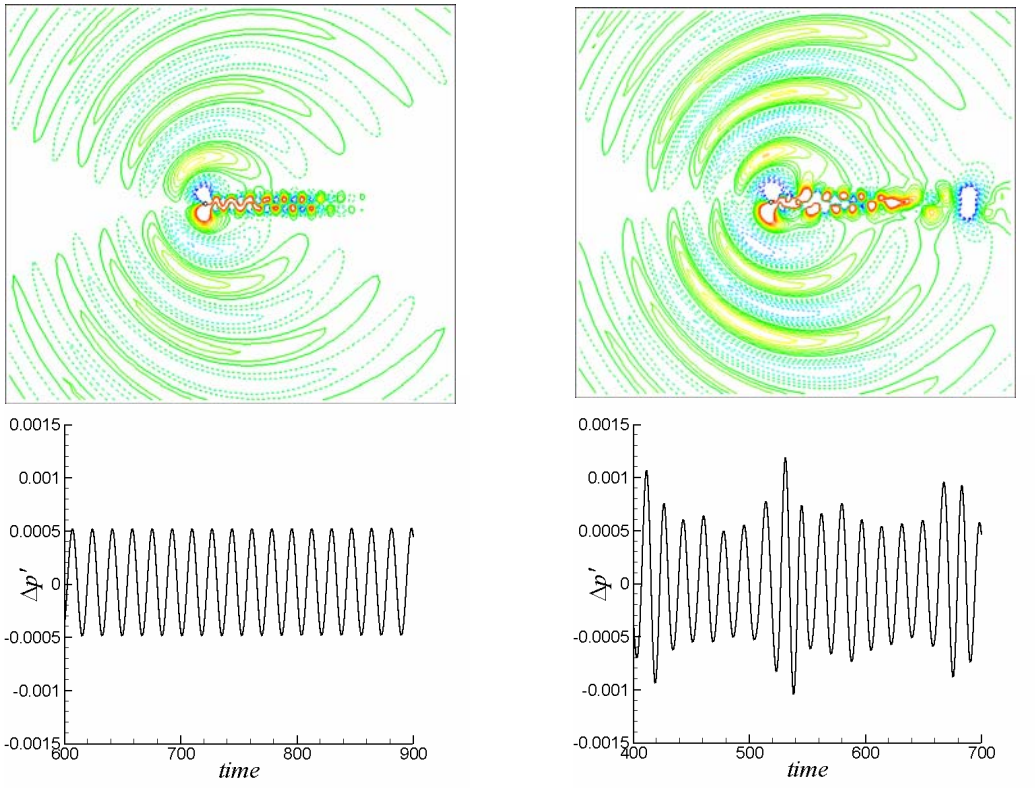

$\Delta p'$ time history at $r = 60D$ and $\Theta = 90^\circ$

Derivation of *P*erturbed *C*ompressible *E*qs. (*PCE*)

- ***Seo* & *Moon*** (*2003, AIAA paper 2003-3270*)

  "A Hybrid Method for Aeroacoustic Noise Prediction of Wall-bounded Shear Flows at Low Mach Numbers", ***will appear in AIAA J. 2005.***

- **Understandings from the *false* solution of *PEE***

$$\rho(x,t) = \rho_0 + \rho'(x,t)$$

$$u_i(x,t) = U_i(x,t) + u_i'(x,t)$$

$$p(x,t) = P(x,t) + p'(x,t)$$

acoustic fluctuations
@ *far-field*

$$\vec{\omega}' = \vec{\nabla} \times \vec{u}' = 0$$

coupling effects (e.g. flow-acoustic)
@ *near-field*

$$\vec{\omega}' = \vec{\nabla} \times \vec{u}' \neq 0$$

A coupling effect becomes important near the wall, when dealing with the noise generated by wall-bounded shear flows, and ***it is associated with*** $\vec{\omega}'$.

Perturbed vorticity transport eq. (*2D*)

$$w = \Omega + w'$$

$$\frac{\partial \Omega}{\partial t} + (\vec{U} \cdot \vec{\nabla})\Omega = \vec{\nabla} \times \vec{F}_{vis,\,I}$$

Incompressible

$$\frac{\partial w}{\partial t} + (\vec{u} \cdot \vec{\nabla})w = -w(\vec{\nabla} \cdot \vec{u}) - \vec{\nabla} \times \left(\frac{1}{\rho}\vec{\nabla}p\right) + \vec{\nabla} \times \vec{F}_{vis,\,C}$$

Compressible

$$\frac{D(w'/\rho)}{Dt} = -\frac{1}{\rho}\left[(\vec{u'} \cdot \vec{\nabla})\Omega + \Omega(\vec{\nabla} \cdot \vec{u'})\right] + \frac{1}{\rho}\vec{\nabla} \times \vec{F}'_{vis} + \frac{1}{\rho}(\vec{\nabla}T \times \vec{\nabla}s)$$

Perturbed

Production by
interaction between incompressible vorticity & perturbed velocities Ω & $\vec{u}'$
(in near-field)

Diffusion by
perturbed viscous stresses (near field)

$$\vec{F}'_{vis} = \vec{F}_{vis,\,C} - \vec{F}_{vis,\,I}$$

Production by
entropy & temperature gradients

Source terms of perturbed vorticity

In *PEE*, *u'* is not zero at the wall, where Ω computed by INS is most intense. So full interactions occur there, contributing to produce ω' without proper diffusion.

Ω *field convection by* $\vec{u}$'

Dilatation rate effect

$$\frac{D(w'/\rho)}{Dt} = -\frac{1}{\rho}\left[(\vec{u}' \cdot \vec{\nabla})\Omega + \Omega(\vec{\nabla} \cdot \vec{u}')\right] + \frac{1}{\rho}\vec{\nabla} \times \vec{F}'_{vis} + \frac{1}{\rho}(\vec{\nabla} T \times \vec{\nabla} s)$$

*important to use a **no-slip** wall B.C to bound* ω' *production*

viscous diffusion of ω'

*important to include **perturbed viscous stresses***

*P*erturbed *C*ompressible *E*qs. (*PCE*)

$$\rho = \rho_o + \rho', \qquad u = U + u', \qquad p = P + p'$$

$$CNS - INS = PCE$$

including the perturbed viscous terms

- $$\frac{\partial \rho'}{\partial t} + \frac{\partial}{\partial x_i}(\rho u'_i + \rho' U_i) = 0$$

- $$\frac{\partial}{\partial t}(\rho u'_i + \rho' U_i) + \frac{\partial}{\partial x_j}\left[u_i(\rho u'_i + \rho' U_i) + \rho_0 U_i u'_j + p'\delta_{ij}\right] = \frac{\partial \tau'_{ij}}{\partial x_j},$$

  where $\tau'_{ij} = \mu_0\left(\partial_j u'_i + \partial_i u'_j - \frac{2}{3}\delta_{ij}\partial_k u'_k\right)$ ← *obtained by assuming* $\mu = \mu_0$ *for* $M < 1$

- $$\frac{\partial p'}{\partial t} + u_j \frac{\partial p'}{\partial x_j} + \gamma p \frac{\partial u'_j}{\partial x_j} = -\frac{DP}{Dt} + (\gamma - 1)\left(\phi - \frac{\partial q_j}{\partial x_j}\right)$$

- **No-slip condition at the wall**

Validation – *INS* + *PCE*

$$\Delta p' = p - \bar{p}$$

DNS

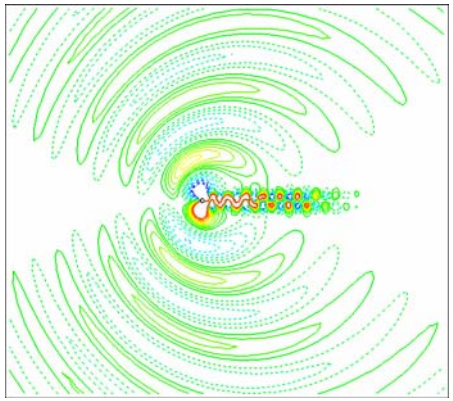

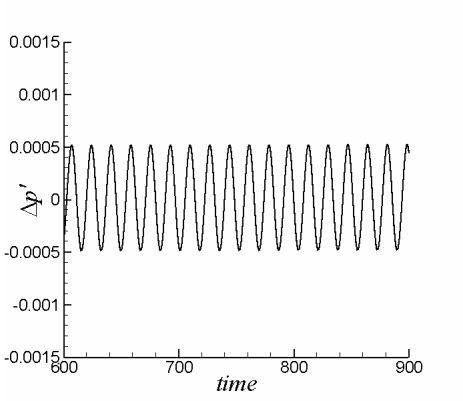

Present (PCE)

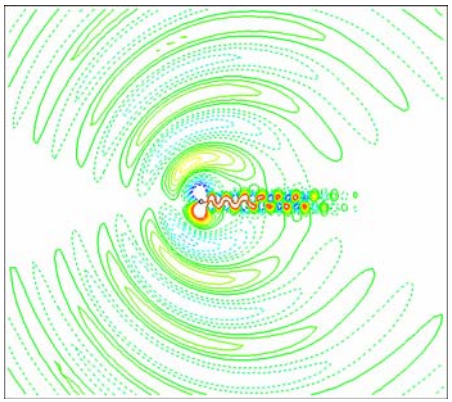

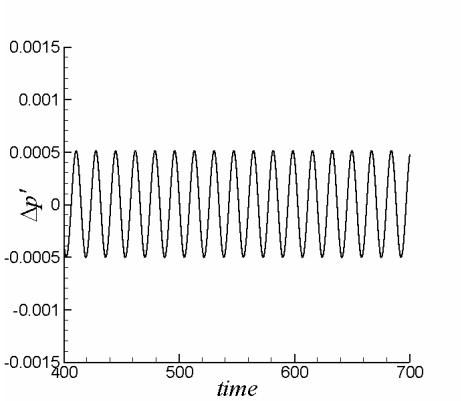

Shen & Sorenson (PEE)

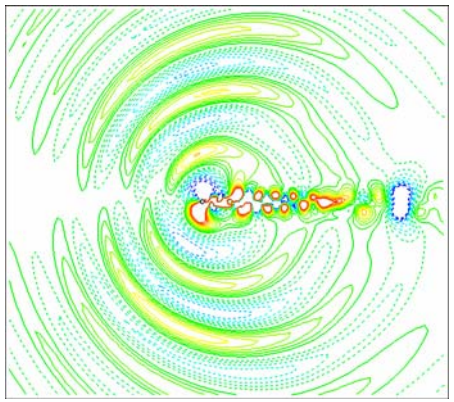

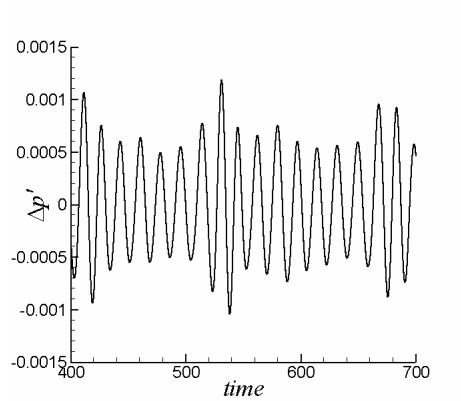

$\Delta p'$ time history at $r = 60D$ and $\Theta = 90^{\circ}$

Validation – pressure fluctuations

$$\Delta p' = p - \bar{p}$$

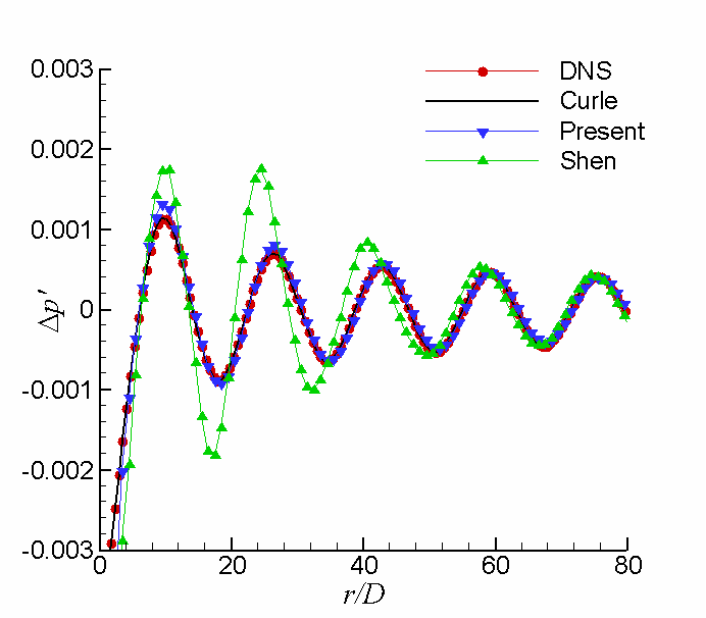

acoustic pressure wave at $x = 0$

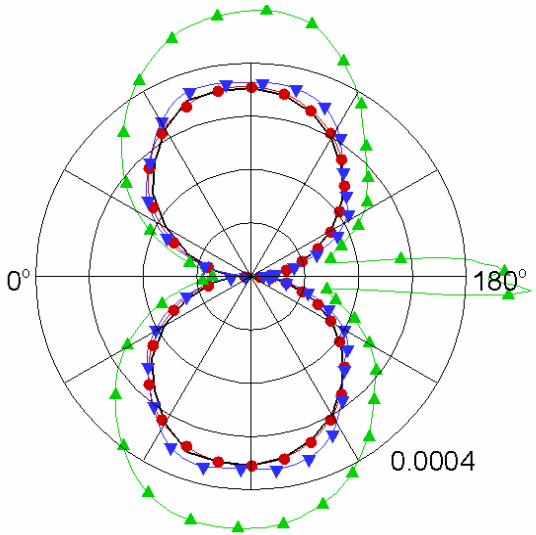

directivity of $\Delta p'_{rms}$ ($r = 60D$)

Validation – vorticity fields

$$w = \Omega + w'$$

DaNS

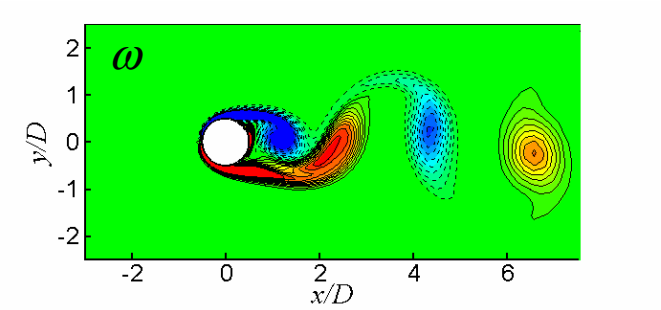

ω' $(\vec{u}'\cdot\vec{\nabla})\Omega$ $\Omega(\vec{\nabla}\cdot\vec{u}')$

Present (PCE)

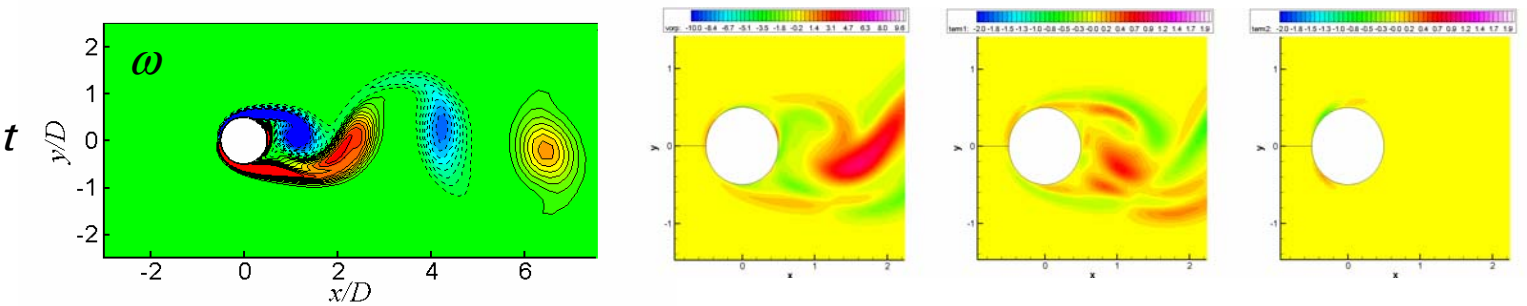

Shen & Sorenson (PEE)

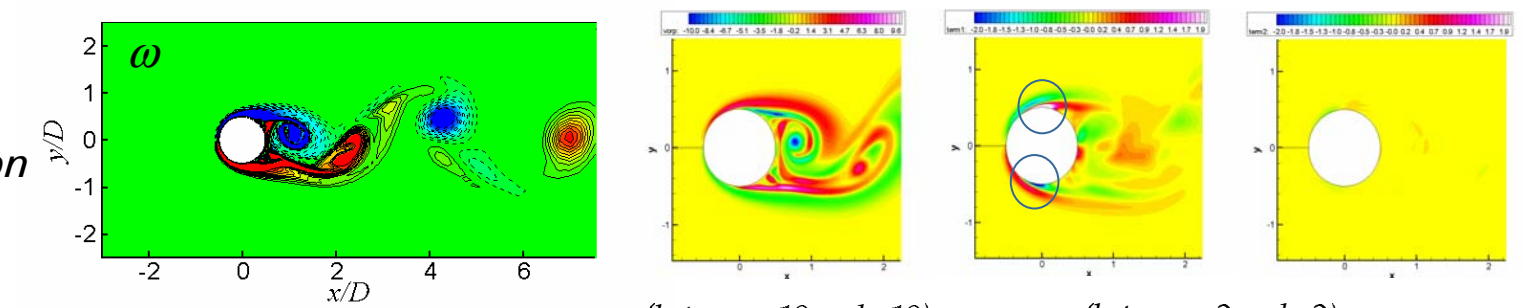

(between -10 and +10) *(between -2 and +2)*

Validation – near-field compressible flow fields (*re-constructed*)

Present (PCE) *DNS*

$p = P + p'$

$\rho = \rho_0 + \rho'$

$T = \gamma \dfrac{(P + p')}{(\rho_0 + \rho')}$

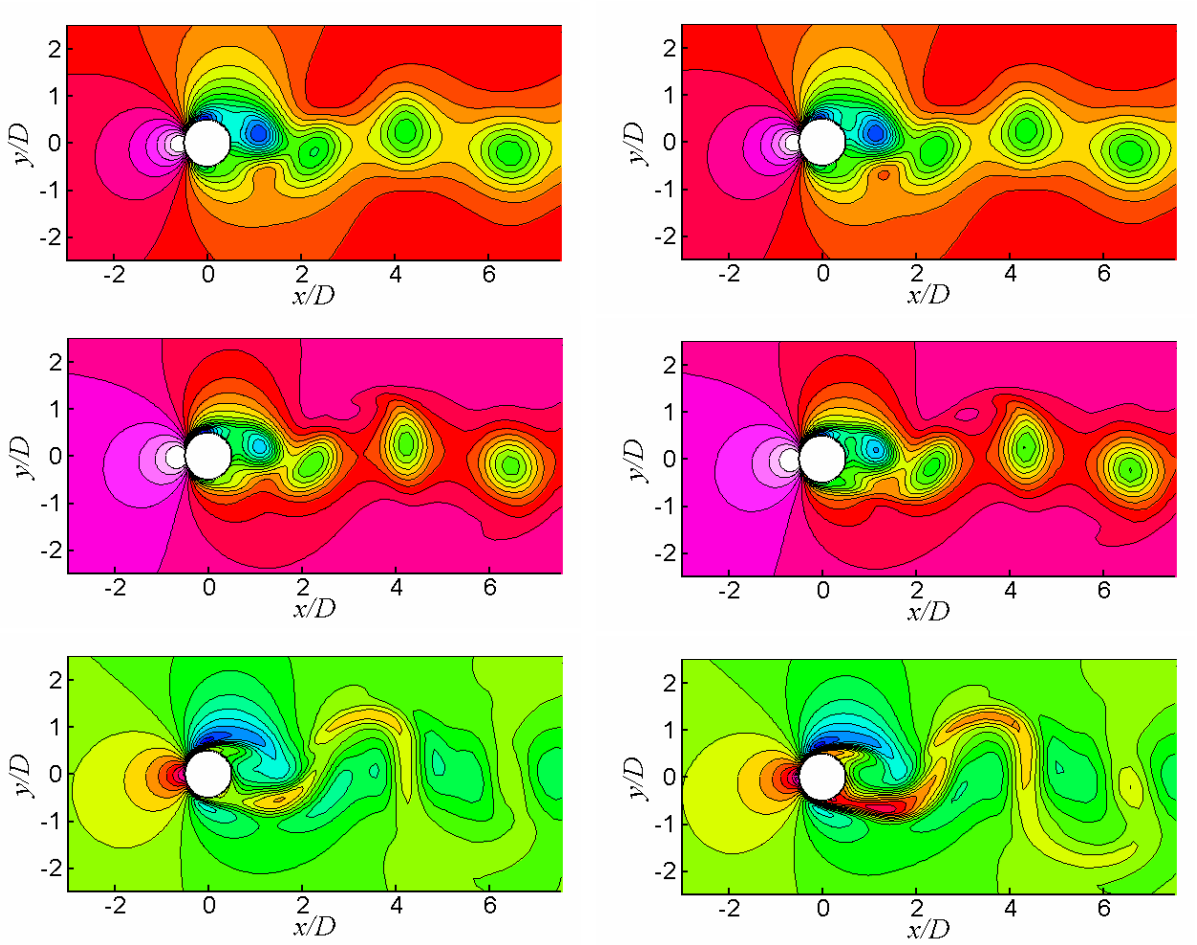

II. Computational Issues of *PCE*

Computational issues of PCE – *efficiency*

- As approach to low Mach number limits,
  - severe restriction on **time step** by numerical stability condition.
- For the turbulent noise prediction,
  - severe restriction on **grid spacing** by flow physics.

→ *Prefer to use different grid systems for flow and acoustic fields* (grid-splitting).

- Increase the **minimum normal grid spacing** near the wall, in order to allow a **larger time step.** $\Delta x_{\min,A} \sim \Delta x_{\min,H} / M_\infty$

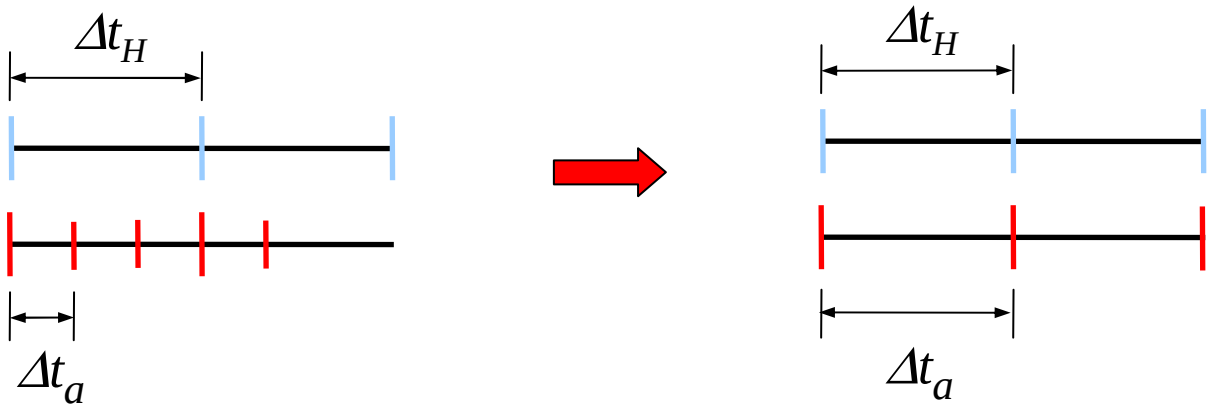

$\Delta x_{\min,A} = \Delta x_{\min,H}$

$\Delta x_{\min,A} \sim \Delta x_{\min,H} / M_\infty$

Cylinder tone (laminar)

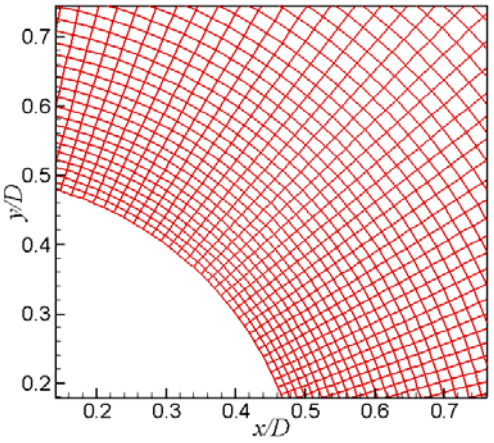

hydrodynamic
(201×201)

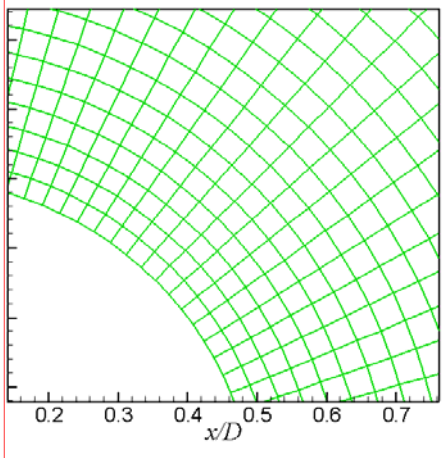

acoustic (coarse)
(121×151)

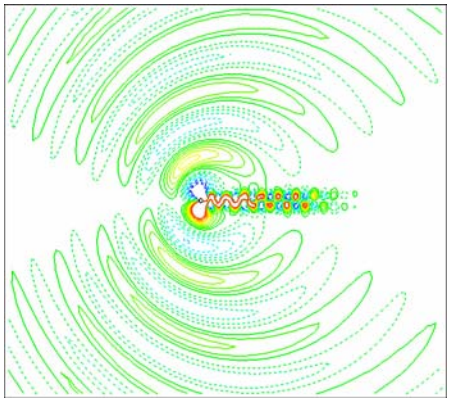

DNS

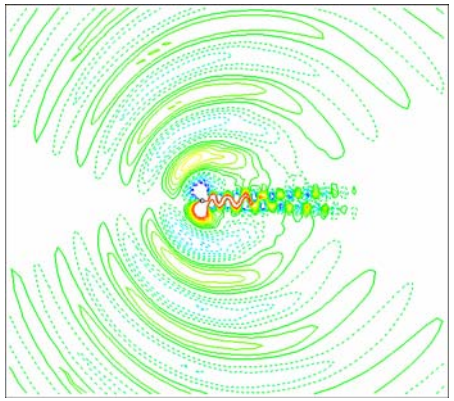

Present (coarse)

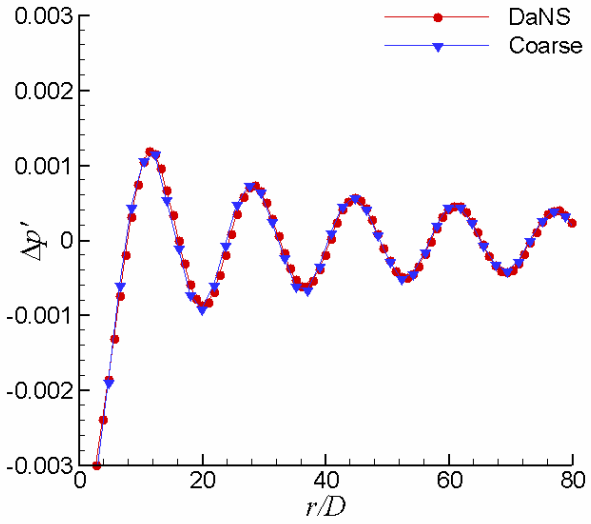

Speed-up factor of PCE, $\Psi_{PCE} = T_{DNS} / T_{PCE}$

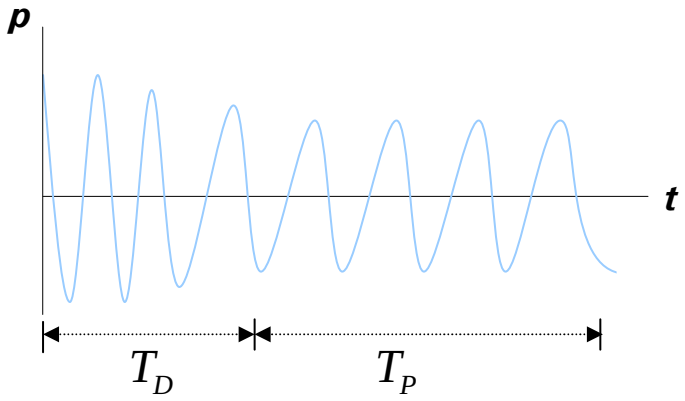

α : T_D / T_P (D: devlp, P: periodic)
N : number of periods
n : number of iterations per period
t_I : CPU time required per iteration
(based on a time step for INS)

$$T_{DNS} = \frac{1}{M_\infty} N n\ t_{I,DNS} + \frac{1}{M_\infty}(\alpha N n\ t_{I,DNS})$$

$$T_{PCE(f)} = \frac{1}{M_\infty} N n\ (t_{I,INS} + t_{I,PCE(f)}) + \alpha N n\ t_{I,INS}$$

$$T_{PCE(c)} = N n\ (t_{I,INS} + t_{I,PCE(c)}) + \alpha N n\ t_{I,INS}$$

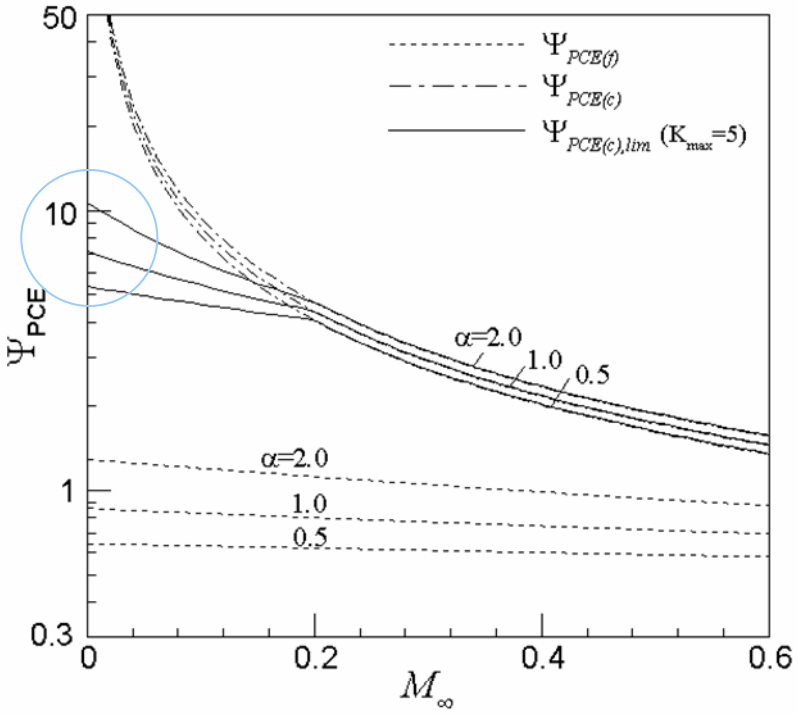

$$\Psi_{PCE(c),\lim} = \frac{(\alpha+1)\, t_{I,DNS}}{(\alpha M_\infty + 1/k)\, t_{I,INS} + (1/k) t_{I,PCE(c)}},$$

where $k = \min(1/M_\infty, K_{\max})$, *Kmax*=5

Computational issues of PCE – *accuracy*

- Vortex (or turbulent eddy) scattering from the trailing-edge:
  - transient transformation from quadruple to dipole

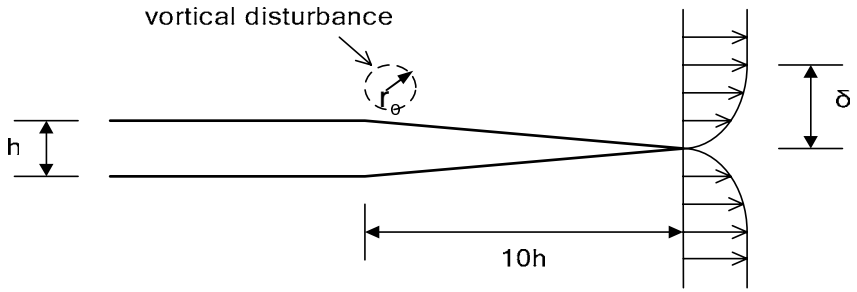

$$\delta = 2.6\,h$$
$$r_0 = 0.5\,h$$
$$V_t = 0.5\,U_\infty$$
$$\mathrm{Re}_h = 2000$$
$$M_\infty = 0.3$$

vortical disturbance

$$u_v^* = V_t (y - y_0) \exp\left(\frac{1-[r/r_0]^2}{2}\right)$$

$$v_v^* = -V_t (x - x_0) \exp\left(\frac{1-[r/r_0]^2}{2}\right)$$

where

$$r = \sqrt{(x-x_0)^2 + (y-y_0)^2}$$

$$(x_0, y_0) = (-8h,\ h)$$

Acoustic grids

grid coarseness factors

$$R_{\min} = \frac{\Delta x_{\min,A}}{\Delta x_{\min,H}} \qquad R_{\delta} = \frac{N_{\delta,H}}{N_{\delta,A}}$$

	N_T	N_δ	R_{min}	R_δ
Fine (*Hydro*)	251×201	26	1	1
Medium	171×161	17	2	1.5
Coarse	116×121	10	4	2.6
Very coarse	101×101	5	10	5.2
Extreme coarse	91×81	3	20	8.6

DP/Dt field projection

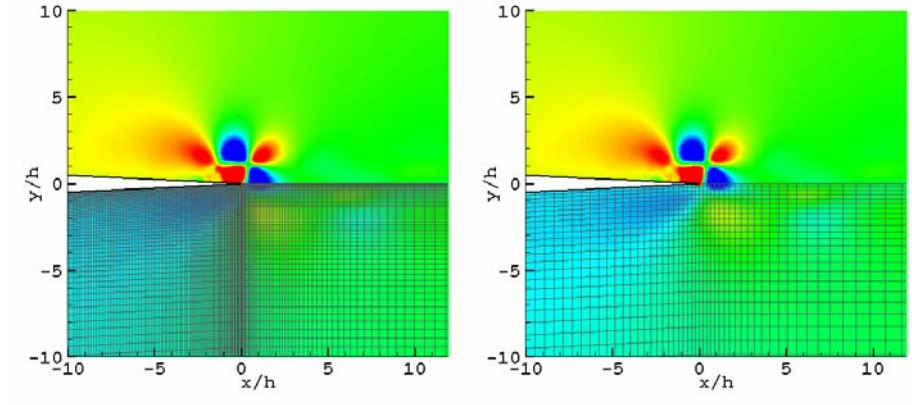

fine coarse

very coarse extremely coarse

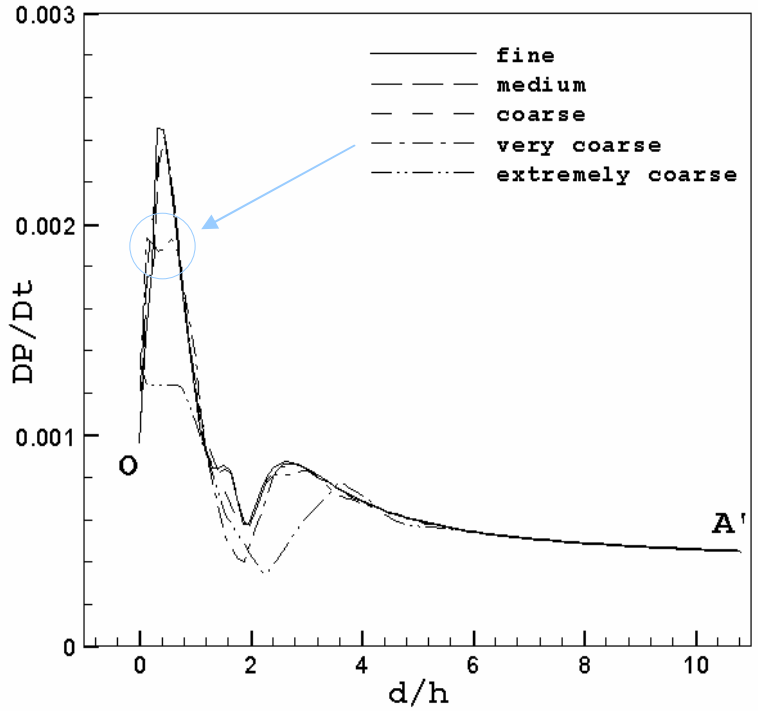

Acoustic pulse strength and $\Delta p'(rms)$ directivity

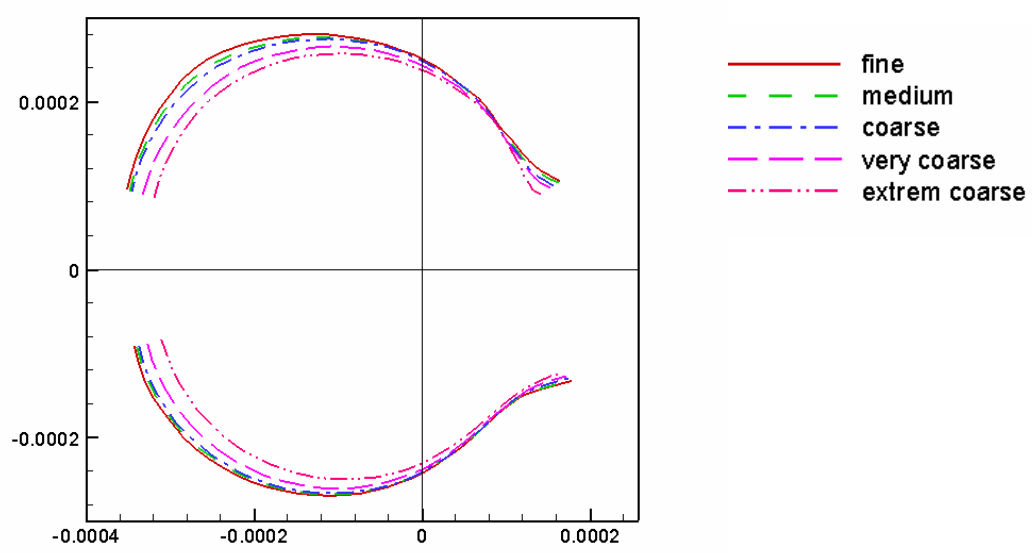

	R_{min}	R_δ	Peak value of $\Delta p'_{rms}$	Relative error	Directivity of $\Delta p'_{rms}$ peak
Fine	1	1	3.67e-4	-	155.1°
Medium	2	1.5	3.63e-4	1.1%	156.4°
Coarse	4	2.6	3.60e-4	1.9%	157.3°
Very coarse	**10**	**5.2**	**3.46e-4**	**5.7%**	**160.2°**
Extreme coarse	**20**	**8.6**	**3.32e-4**	**9.5%**	**162.6°**

III. Linearized Perturbed Compressible Equations (*LPCE*) – $M \lll 1$

Instability of perturbed vorticity (ω′)

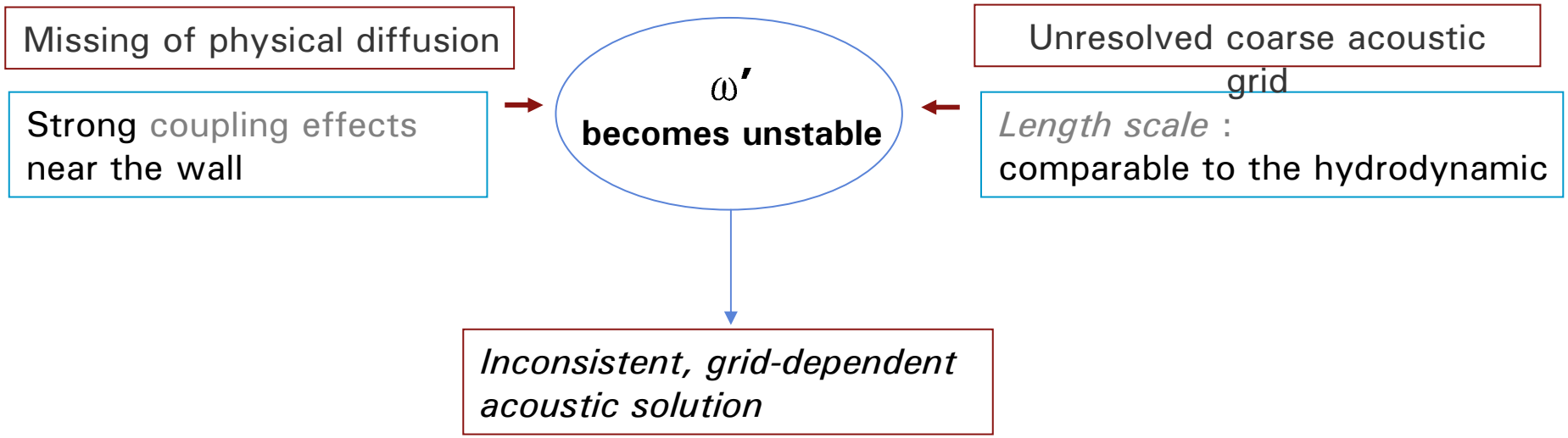

At low Mach numbers,
the effect of perturbed vorticity is negligible for the noise generation.

Exclude the errors caused by perturbed vorticity by suppressing the generation of perturbed vorticity !

*P*erturbed *C*ompressible *E*qs. (*PCE*)

- $$\frac{\partial \rho'}{\partial t} + \frac{\partial}{\partial x_i}(\rho u'_i + \rho' U_i) = 0$$

- $$\frac{\partial}{\partial t}(\rho u'_i + \rho' U_i) + \frac{\partial}{\partial x_j}\left[u_i(\rho u'_i + \rho' U_i) + \rho_0 U_i u'_j + p'\delta_{ij}\right] = \frac{\partial\, \tau'_{ij}}{\partial\, x_j},$$

- $$\frac{\partial p'}{\partial t} + u_j \frac{\partial p'}{\partial x_j} + \gamma p \frac{\partial u'_j}{\partial x_j} = -\frac{DP}{Dt} + (\gamma - 1)\left(\phi - \frac{\partial q_j}{\partial x_j}\right)$$

$$where \quad \tau'_{ij} = \mu_0\left(\partial_j u'_i + \partial_i u'_j - \frac{2}{3}\delta_{ij}\partial_k u'_k\right)$$

- **No-slip condition at the wall**

Derivation of LPCE formulation

- Neglecting the second-order, non-linear terms

$$\frac{\partial \rho'}{\partial t} + (\vec{U} \cdot \nabla)\rho' + \rho_0(\nabla \cdot \vec{u}') = 0$$

$$\frac{\partial \vec{u}'}{\partial t} + \nabla(\vec{u}' \cdot \vec{U}) + \frac{1}{\rho_0}\nabla p' = -(\vec{\Omega} \times \vec{u}') - (\vec{\omega}' \times \vec{U}) - \frac{\rho'}{\rho_0}\frac{D\vec{U}}{Dt} + \frac{1}{\rho_0}\vec{f}'_{vis}$$

Mathematical identity

$$(\vec{U} \cdot \nabla)\vec{u}' + (\vec{u}' \cdot \nabla)\vec{U} = \nabla(\vec{u}' \cdot \vec{U}) + (\vec{\Omega} \times \vec{u}') + (\vec{\omega}' \times \vec{U})$$

$$\frac{\partial p'}{\partial t} + (\vec{U} \cdot \nabla)p' + \gamma P(\nabla \cdot \vec{u}') + (\vec{u}' \cdot \nabla)P = -\frac{DP}{Dt} + (\gamma - 1)\left(\Phi - \nabla \cdot \vec{q}\right)$$

Perturbed vorticity transport eq. (*3D*)

$$\frac{\partial}{\partial t}\left(\frac{\vec{\omega}'}{\rho}\right)+(\vec{u}\cdot\nabla)\left(\frac{\vec{\omega}'}{\rho}\right)=\frac{1}{\rho}\left[(\vec{\Omega}\cdot\nabla)\vec{u}'+(\vec{\omega}'\cdot\nabla)\vec{u}\right]-\frac{1}{\rho}\left[(\vec{u}'\cdot\nabla)\vec{\Omega}+\vec{\Omega}(\nabla\cdot\vec{u}')\right]+\frac{1}{\rho^3}(\nabla\rho\times\nabla p)+\frac{1}{\rho}\nabla\times\vec{F}_{vis}$$

$$\frac{\partial\vec{u}'}{\partial t}+\nabla(\vec{u}'\cdot\vec{U})+\frac{1}{\rho_0}\nabla p'=-(\vec{\Omega}\times\vec{u}')-(\vec{\omega}'\times\vec{U})-\frac{\rho'}{\rho_0}\frac{D\vec{U}}{Dt}+\frac{1}{\rho_0}\vec{f}'_{vis}$$

Sources to the perturbed vorticity generation

*L*inearized *P*erturbed *C*ompressible *E*qs. (LPCE) - M<<<1

- Linearized to the base incompressible flow field

$$\frac{\partial \rho'}{\partial t} + (\vec{U} \cdot \nabla)\rho' + \rho_0(\nabla \cdot \vec{u}') = 0$$

$$\frac{\partial \vec{u}'}{\partial t} + \nabla(\vec{u}' \cdot \vec{U}) + \frac{1}{\rho_0}\nabla p' = 0 \quad \longrightarrow \quad \boxed{\frac{\partial \omega'}{\partial t} = 0}$$

$$\frac{\partial p'}{\partial t} + (\vec{U} \cdot \nabla)p' + \gamma P(\nabla \cdot \vec{u}') + (\vec{u}' \cdot \nabla)P = \boxed{-\frac{DP}{Dt}}$$

Only explicit noise source at low Mach numbers
Goldstein(2003), Ewert & Schröder (2003)

Numerical test problems

1. Dipole tone noise form a circular cylinder at Re = 150, M = 0.1

   - Basic validation by comparing with ***DNS***

2. Quadruple noise generated by the Kirchhoff vortex

   - Fundamental vortex sound problem, comparing with the ***exact solution***

3. Sound radiated from a temporal mixing layer

   - Model for ***turbulent noise*** prediction, practical vortex sound problem

1. Tonal noise from a circular cylinder

- Tonal noise from a circular cylinder at $M_\infty = 0.1$, $Re_D = 150$ ($\Delta p'$)

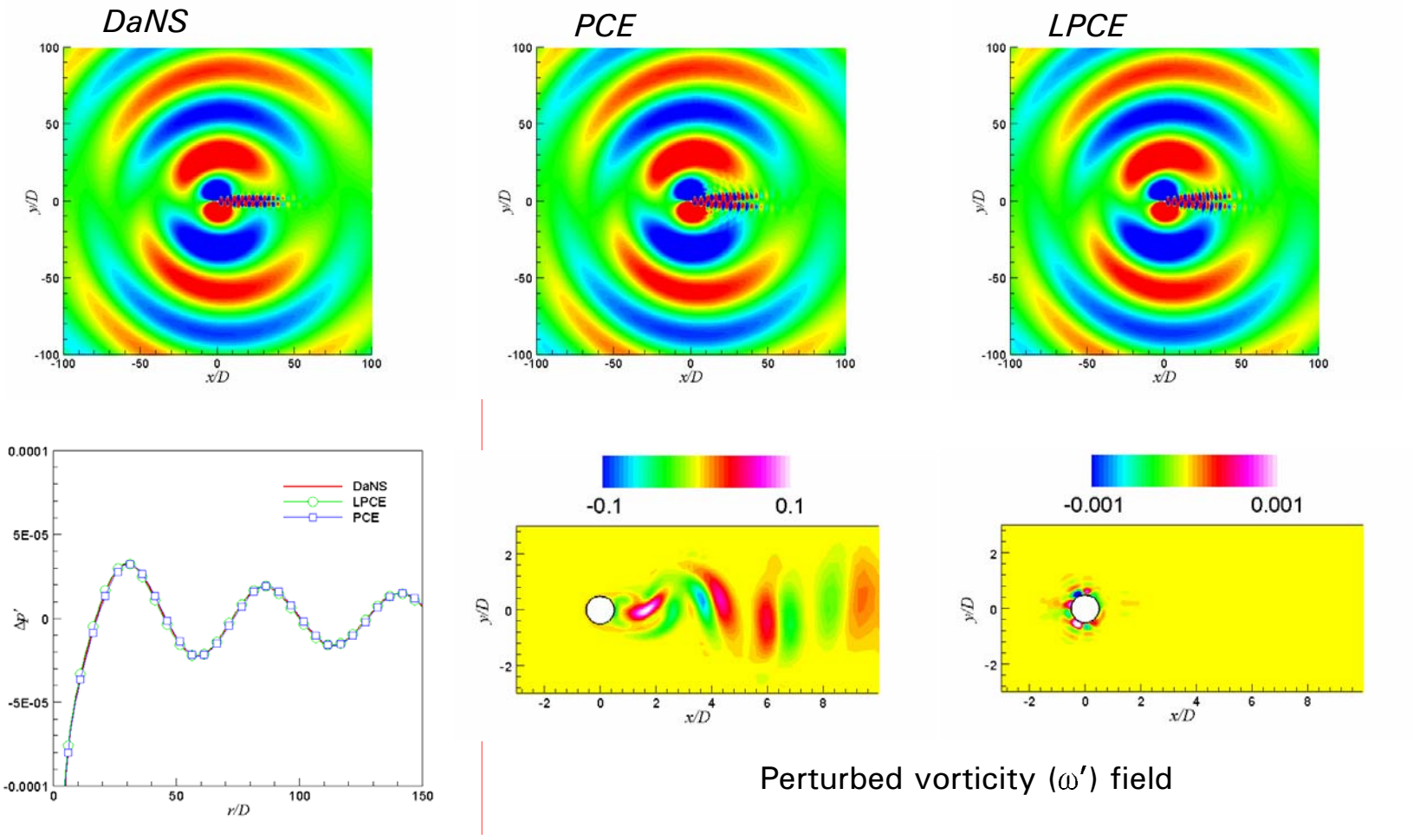

Perturbed vorticity (ω') field

2. Quadruple noise generated by the Kirchhoff vortex

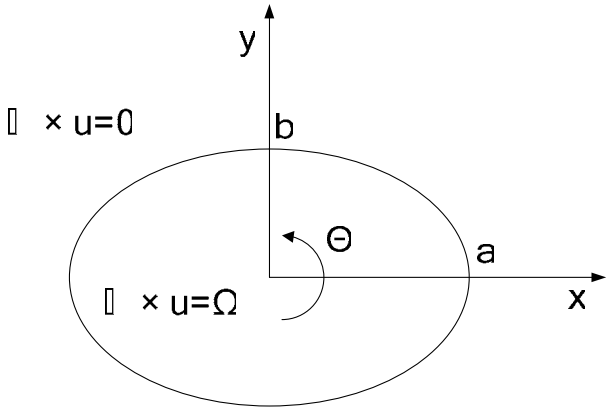

Kirchhoff vortex

$$\Theta = \frac{ab}{(a+b)^2}\Omega$$

$$M_\Theta = \frac{(a+b)\Theta}{c} = 0.1$$

Acoustic grid resolution

	Fine	Coarse
Kirchhoff vortex core	100×100	10×10

2. Quadruple noise generated by the Kirchhoff vortex

no perturbed vorticity generation

PCE (*fine*)

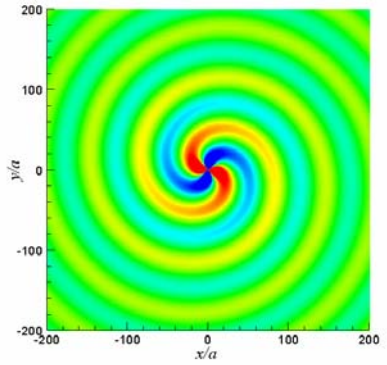

LPCE (*fine*)

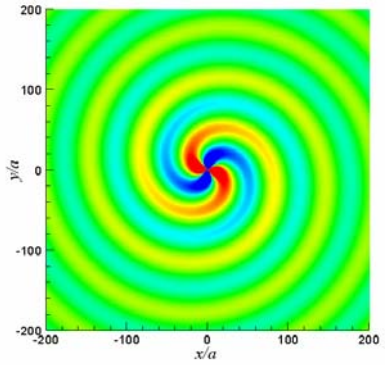

PCE (*coarse*)

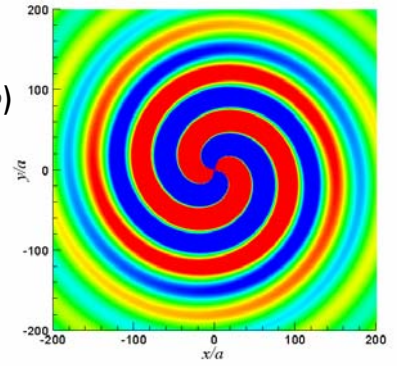

LPCE (*coarse*)

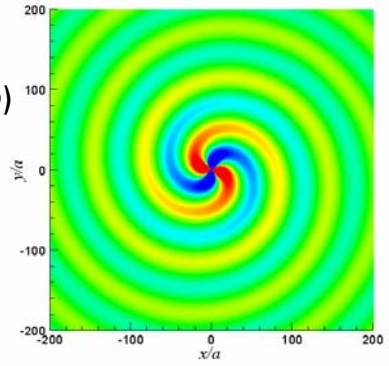

Pressure fluctuation ($\Delta p'$) fields

Instantaneous pressure fluctuation along the $y = 0$ line

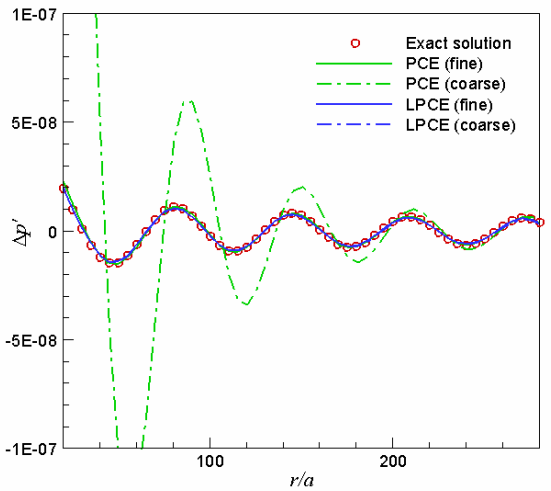

Exact solution by Müller (1998)

Acoustic solution is corrupted by falsely resolved perturbed vorticity!

2. Quadruple noise generated by the Kirchhoff vortex

Most dominant source for the perturbed vorticity (ω′) generation : $(\vec{u}\,' \cdot \nabla)\Omega$

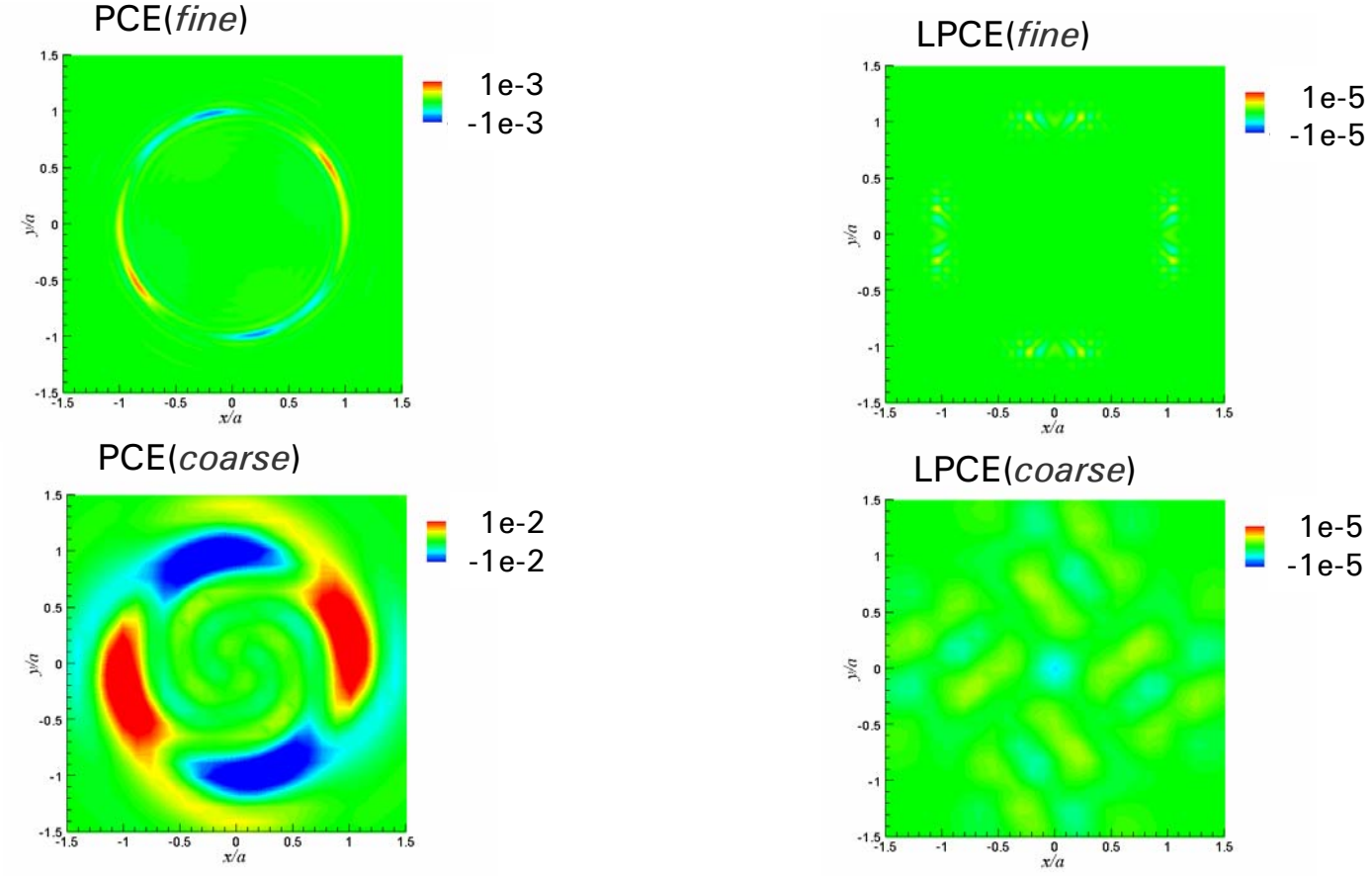

Perturbed vorticity (ω′) fields

3. Sound radiated from a temporal mixing layer

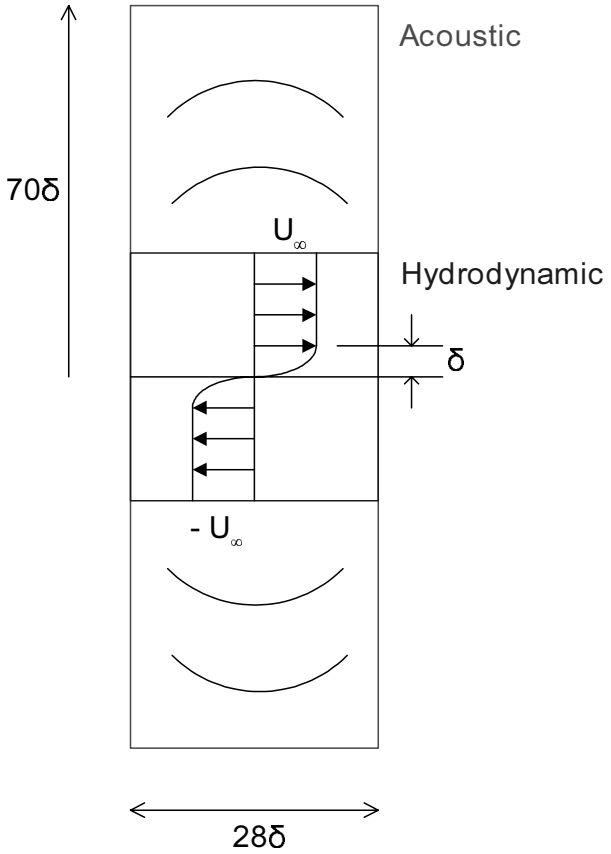

$$M_s = \frac{2U_\infty}{c} = 0.1$$

$$\mathrm{Re}_\delta = 10000$$

Acoustic grid resolution

	Fine	Coarse
Hydrodynamic domain	200×200	40×40

3. Sound radiated from a temporal mixing layer

- The evolution of vortical field (Ω)

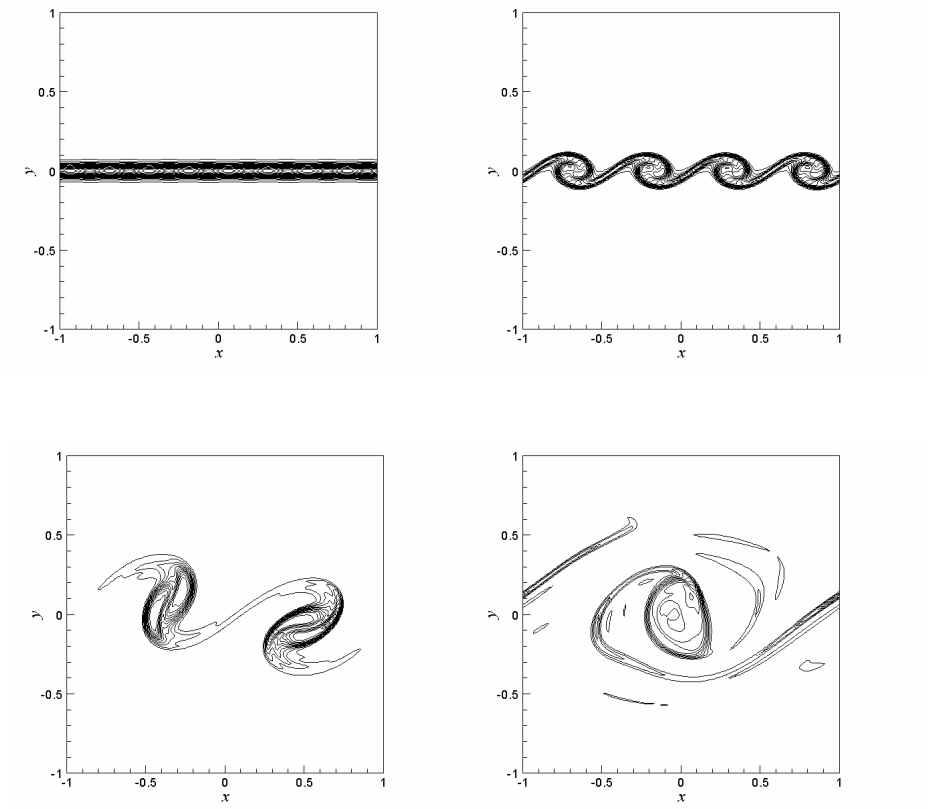

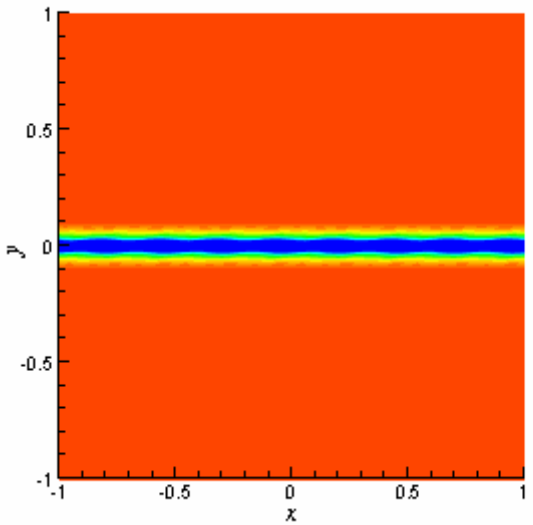

3. Sound radiated from a temporal mixing layer

Hydrodynamic vorticity (Ω)

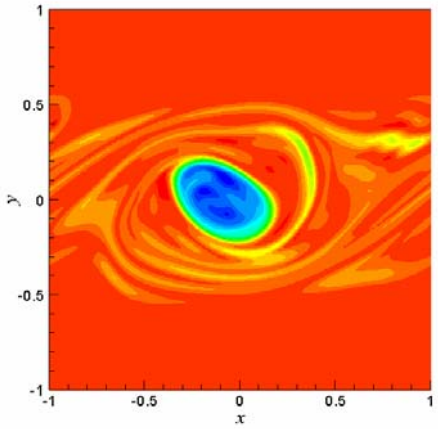

Perturbed vorticity (ω')

PCE (*fine*)

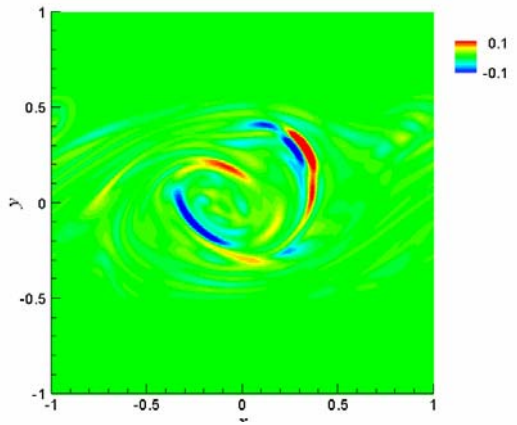

PCE (*coarse*)

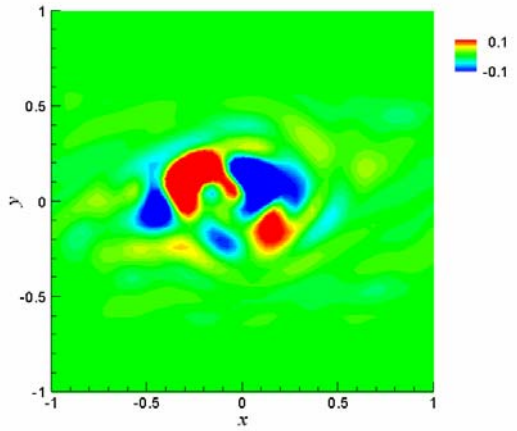

3. Sound radiated from a temporal mixing layer

- Acoustic fields ($\Delta p'$)

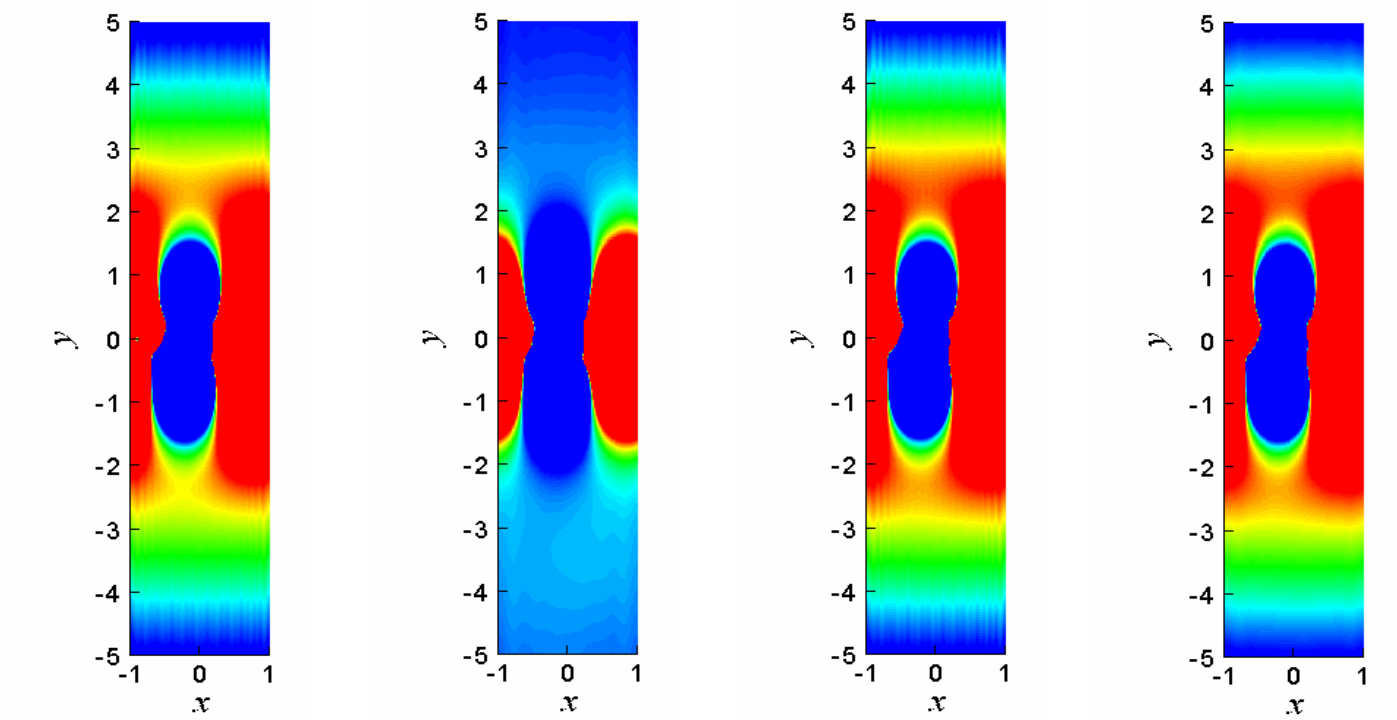

PCE (*fine*) | PCE (*coarse*) | LPCE (*fine*) | LPCE (*coarse*)

3. Sound radiated from a temporal mixing layer

- Time histories of instantaneous pressure fluctuation ($\Delta p'$) at (0, 56δ)

PCE

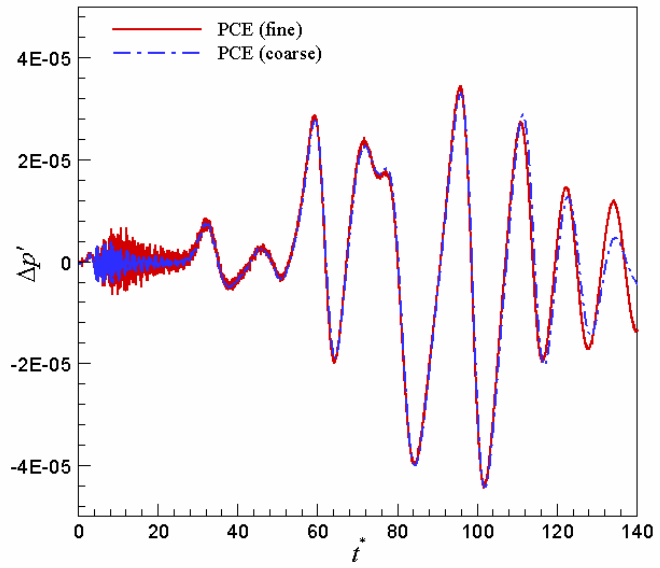

LPCE

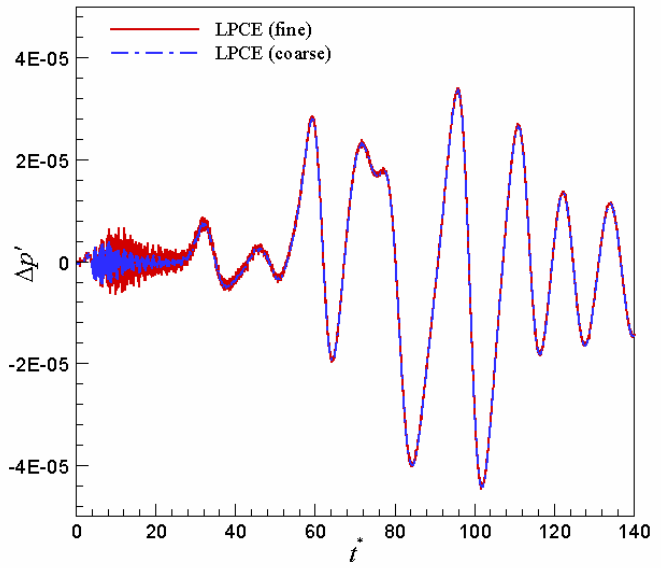

Concluding Remarks

- The perturbed vorticity is not a *major* contributor in acoustic wave generation at low Mach numbers.
- The perturbed vorticity could be a source of unwanted errors on the *unresolved grid*.
- The *'Linearized Perturbed Compressible Equations'* in which the generation of perturbed vorticity is *suppressed*, are proposed.
- The consistent, grid-independent acoustic solution is secured by the *LPCE formulation*.
- The formulation may be useful for the *turbulent noise prediction at low Mach numbers*.

Computational Aeroacoustics

for

Low Mach Number Flows (II)

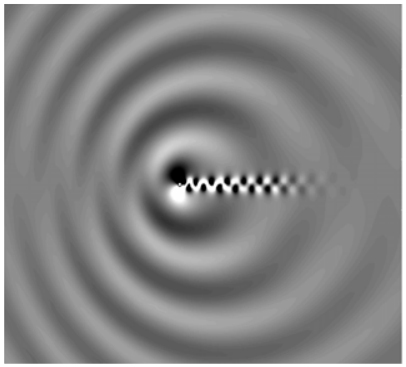

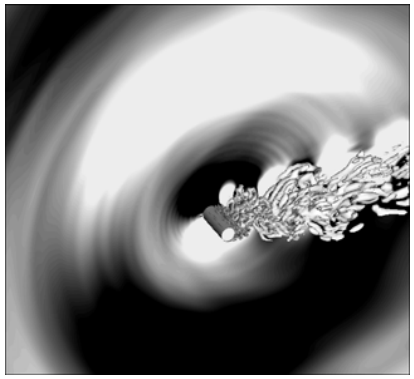

Young J. Moon

Korea University
Department of Mechanical Engineering
Seoul, Korea

Contents

III. 3D Flow past a Circular Cylinder at $Re_D = 46000$ & $M = 0.21$

3D Flow past a circular cylinder at $Re_D = 46000$ & $M = 0.21$

- $Re_D = 46000$: sub-critical regime ($1{,}000 < Re_D < 200{,}000$).
- A boundary layer remains laminar but the shear layer exhibits immediate transition to turbulence.
- It produces a broadened tone at vortex shedding frequency as well as broadband noise due to wake turbulences.
- Spanwise correlation length is about $2.7D$ (Szepessy, 1994).

Incompressible LES

- Filtered incompressible Navier-Stokes equaions.

$$\frac{\partial \tilde{U}_j}{\partial x_j} = 0$$

$$\rho_0 \frac{\partial \tilde{U}_i}{\partial t} + \rho_0 \frac{\partial}{\partial x_j}(\tilde{U}_i \tilde{U}_j) = -\frac{\partial \tilde{P}}{\partial x_i} + \mu_0 \frac{\partial}{\partial x_j}\left(\frac{\partial \tilde{U}_i}{\partial x_j} + \frac{\partial \tilde{U}_j}{\partial x_i} \right) - \rho_0 \frac{\partial}{\partial x_j} M_{ij}$$

- Smagorinsky sub-grid model with Van Driest wall damping function:
  Smagorinsky constant ***Cs = 0.065***

$$M_{ij} = \widetilde{U_i U_j} - \tilde{U}_i \tilde{U}_j$$

$$= -\{(0.065)(1 - \exp(y^+ / 25)^3)^{1/2} \Delta\}^2 \left|\tilde{S}\right| \tilde{S}_{ij}$$

- No model **New Calc.**

Computational methods for *iLES*

- Iterative fractional step method.
- A sixth-order compact finite difference scheme for spatial discretization.
- 3-stage Runge-Kutta method for time integration.
- Spanwise domain size, $L_s = 3D$.
- Uniform inflow condition / Periodic spanwise boundary condition.
- O-grid with $181 \times 181 \times 31 (= 0.97 \text{x} 10^6)$ points.

Turbulent flow field

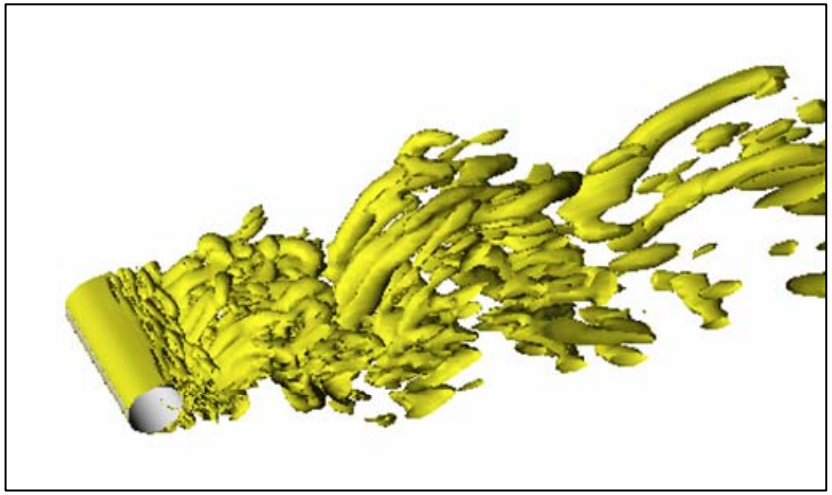

Iso-surfaces of Q = 0.5

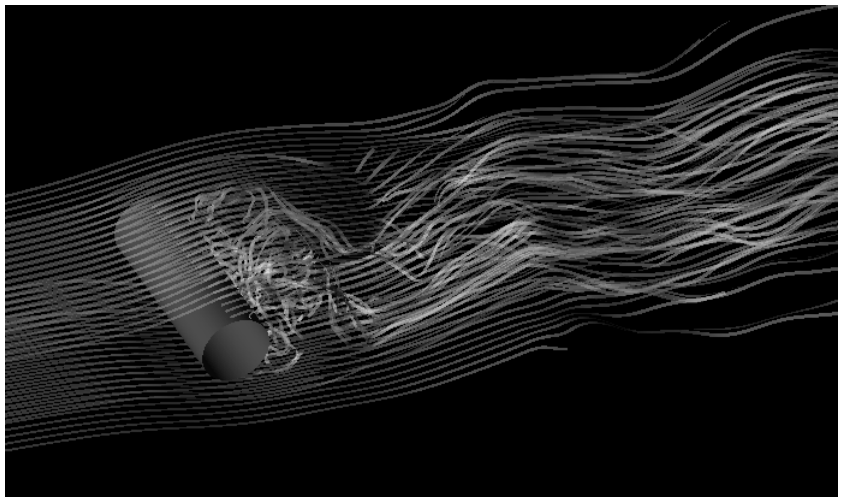

Streamtraces

Highly three-dimensional wake structure and coherent Karman vortex street.

Validation – *iLES* (Smagorinsky)

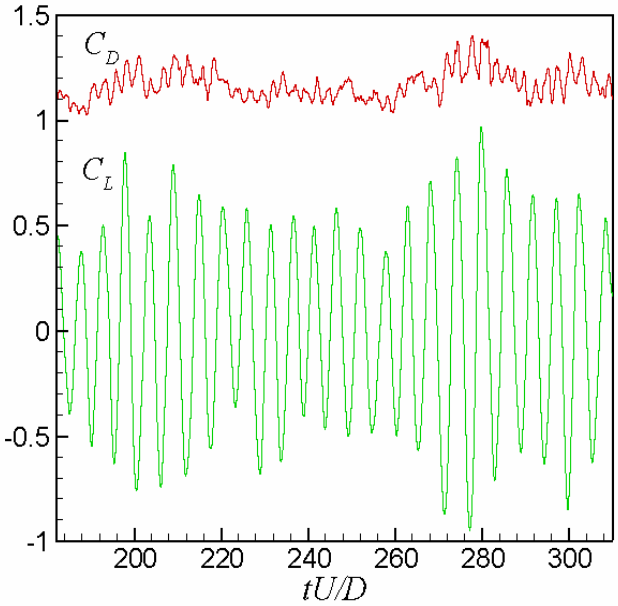

Time histories of drag and lift coefficients

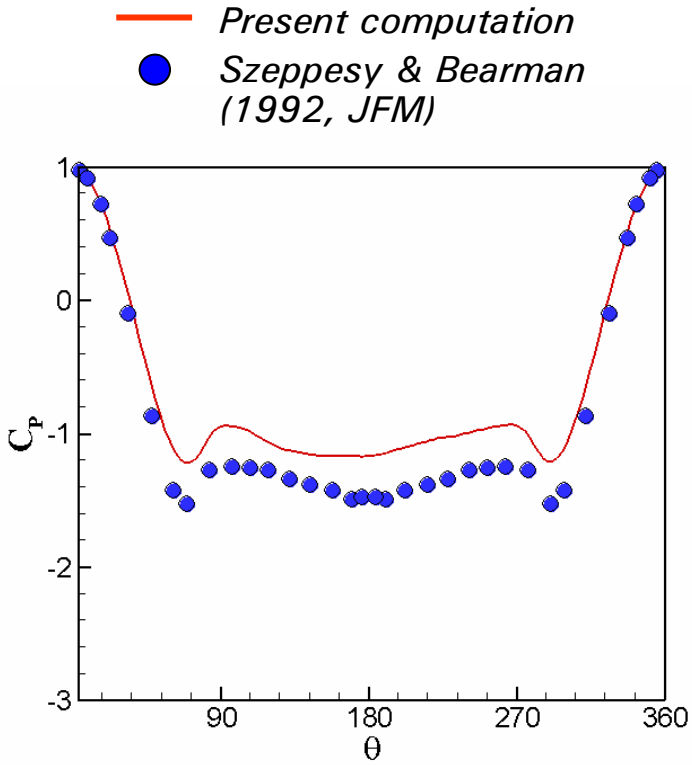

Mean pressure coefficient at the wall

Validation – Mean & Fluctuating data

	Present LES (Smagorinsky)	Experiement (*Szepessy* & *Bearman*)
St	0.19	0.19
$C_{D,avg}$	1.15	1.35
$C_{D}{}'_{rms}$	0.067	0.16
$C_{L}{}'_{rms}$	0.44	0.45-0.5

3D PCE

- Acoustic measurement($r = 185D$): *Boudet et al. (AIAA 2003-3217).*
- Acoustic domain: extended to $r = 200D$.
- Spanwise domain: same as *LES* ($L_s = 3D$).
- Wavelength($St \sim 0.19$): about $25D$.
- Very narrow domain: $L_s/\lambda \approx 0.12$ and $r/L_s \approx 66$.

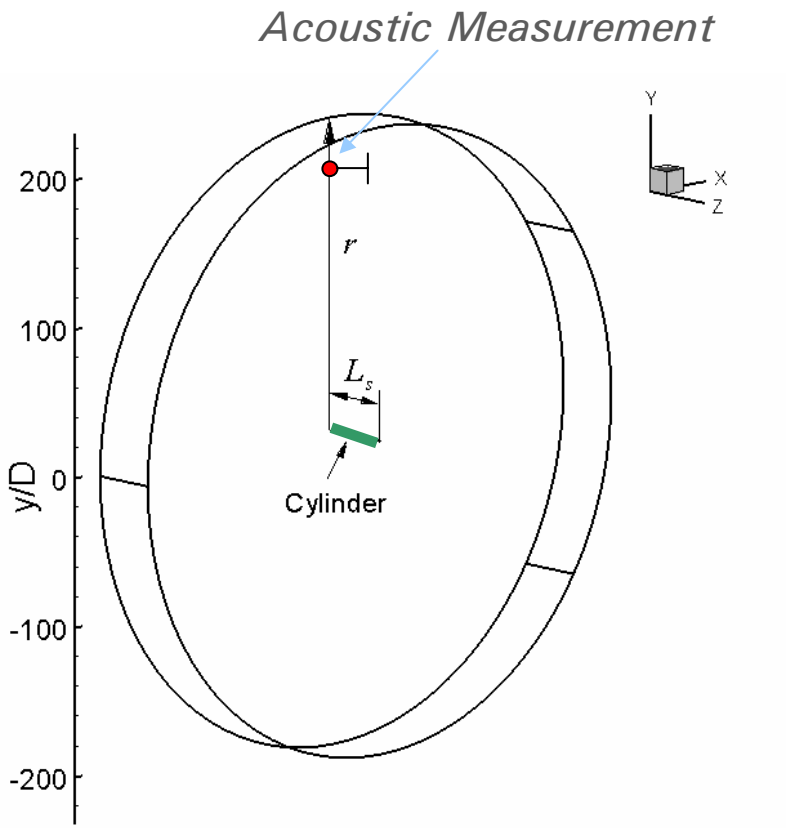

acoustic domain

Acoustic grid

- 121×181×11(= 0.24×10^6) points.
- 1.5 times coarser in *r-dir*.
- minimal grid spacing at the wall:
  5 times larger than the hydro-grid.
- acoustic calculation:
  with same time step used for
  incompressible LES,
  5 times larger than DaNS.

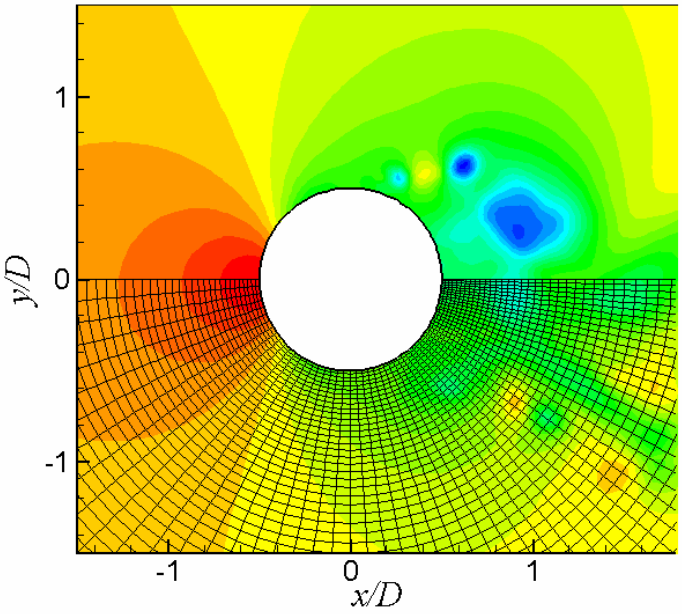

acoustic grid &
interpolated static pressure field

Explicit source term

- magnitude of the explicit source term, $\left| D\tilde{P} / Dt \right|$

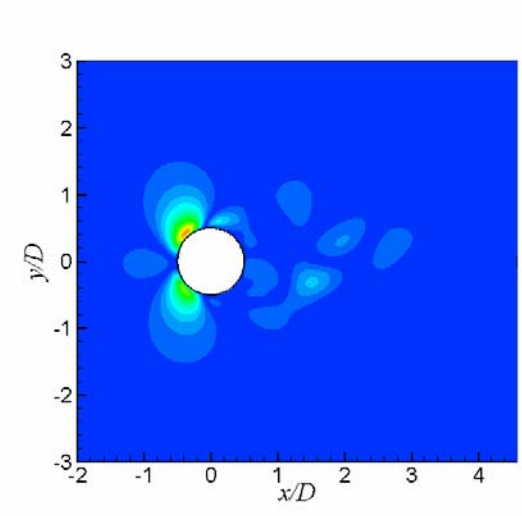

$Re_D = 200$ (INS)

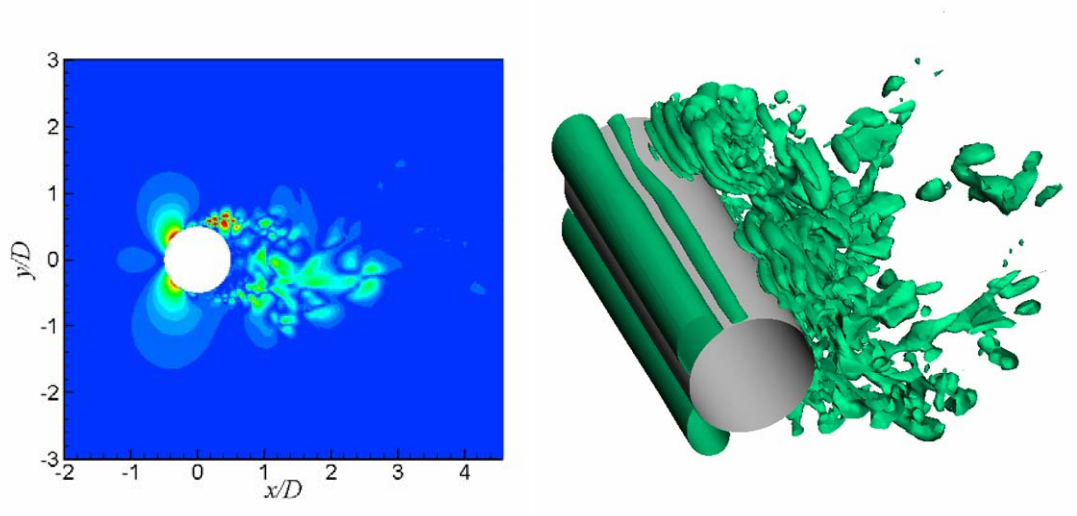

$Re_D = 46000$ (LES)

Periodic BC v.s. Absorbing BC

- Spanwise boundary condition for 3D acoustic simulation of cylindrical problems.

  - Periodic boundary condition
    - Unphysically correlated acoustic solution for a small span.

  - Absorbing (non-reflecting) boundary condition
    - Simulating 3D noise radiation from a small span.
    - Does an absorbing boundary condition, however, work properly for narrow domains *(e.g.* $r / Ls >> 1$ *) ?*

3D Acoustic Wave Propagation in a Narrow Domain

$$U = V = W = 0$$

$$P(\vec{x},t) = P_{\infty} + 0.1\sin(2\pi\lambda t)\exp\left(-\frac{x^2+y^2+z^2}{25}\right)$$

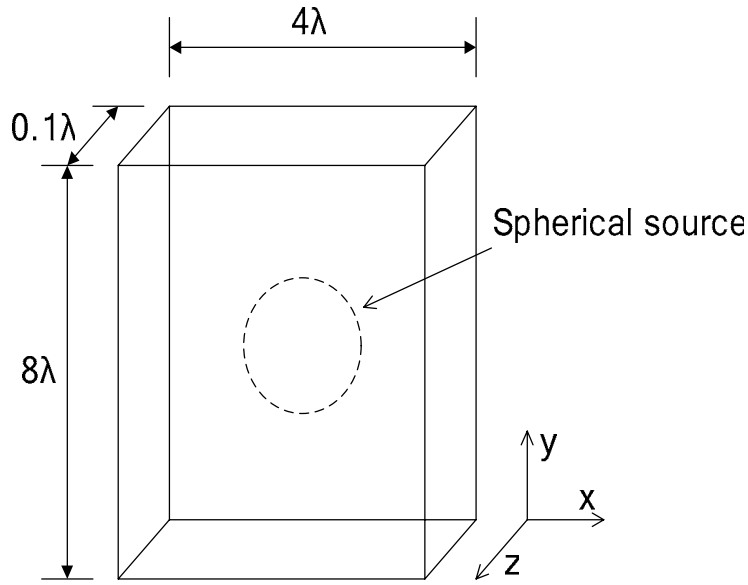

schematic of numerical exp.

To verify the ETA BC, a numerical experiment is set up.

- A spherical harmonic acoustic source .
- Aspect ratio is about *r/Ls* = 80 in *yz-plane*.
- Acoustic grid: 41×81×11 points.
- PCE is solved with a zero convectional velocity.

Computational Results

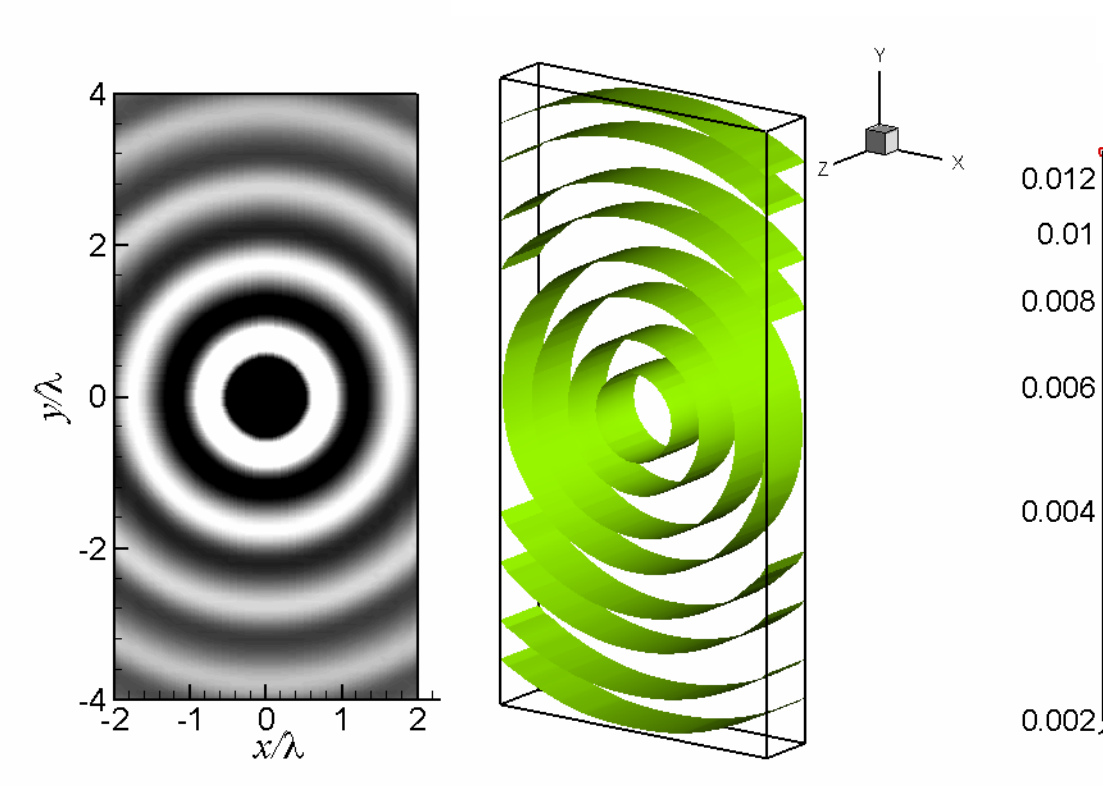

Contours & Iso-surfaces of pressure fluctuation; z-axis is magnified by 8 times

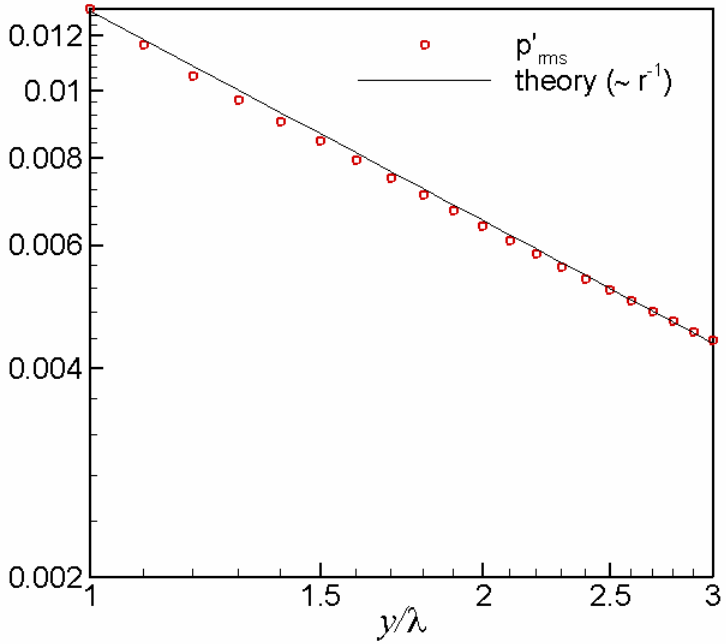

Acoustic wave strength along the y-axis

Pressure fluctuation field

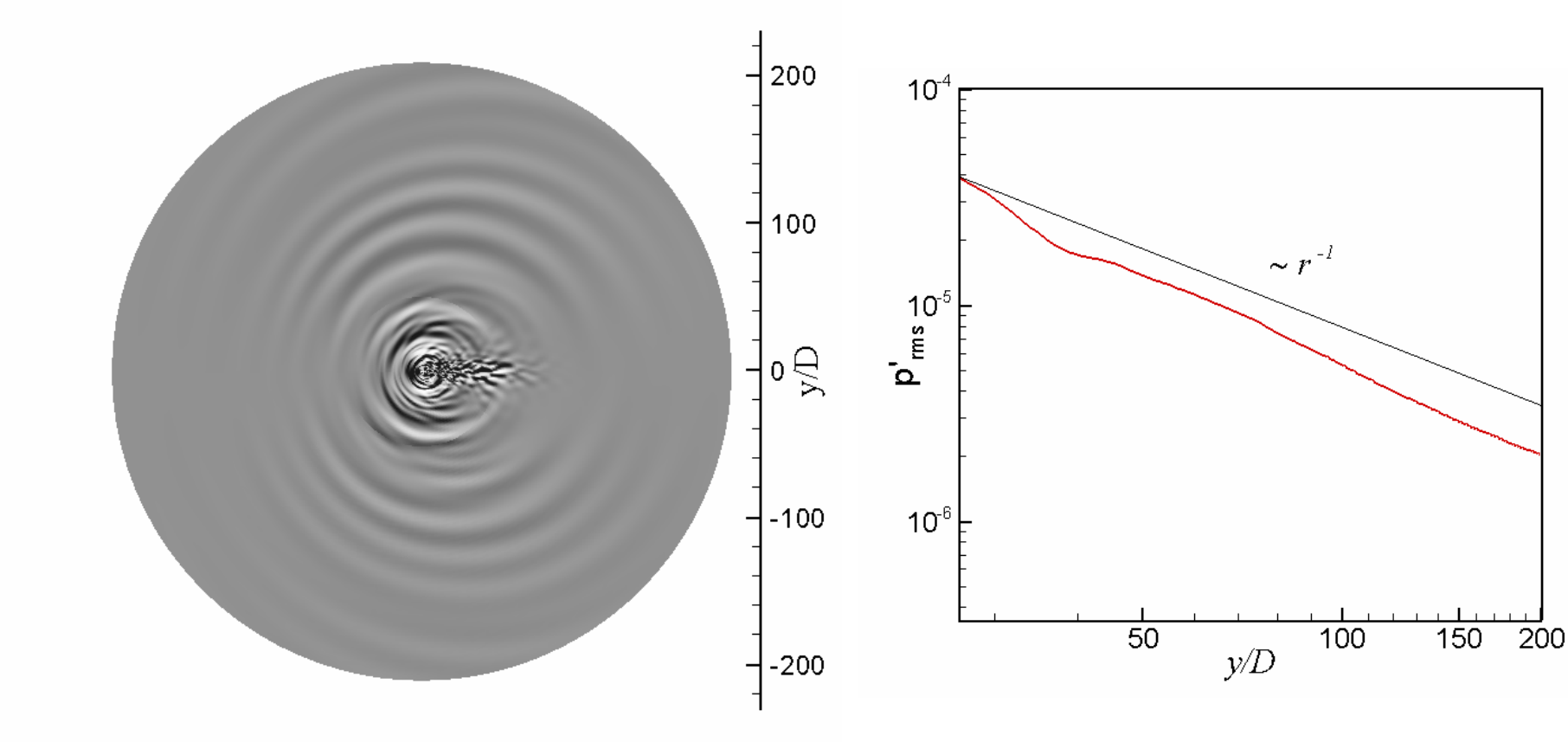

Acoustic pressure signal & SPL spectrum

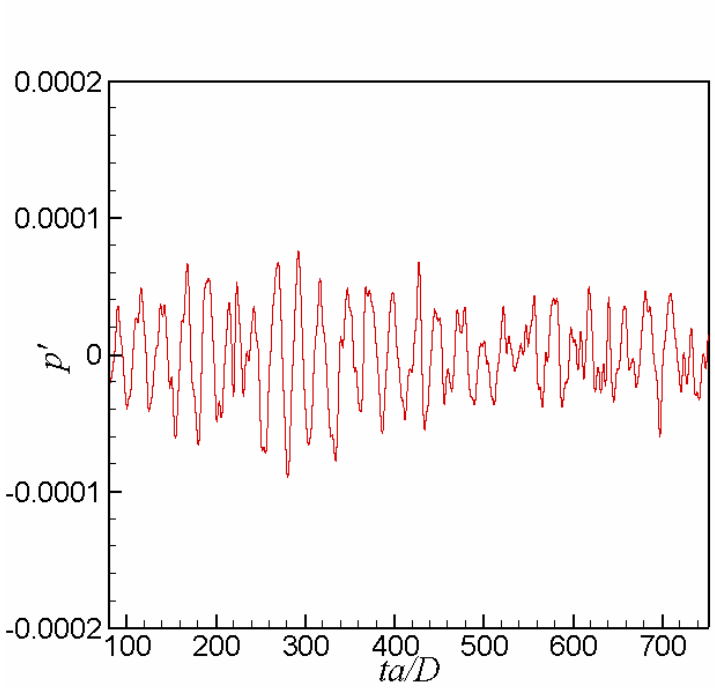

Time history of fluctuating pressure at $r = 30D$ directly above the cylinder

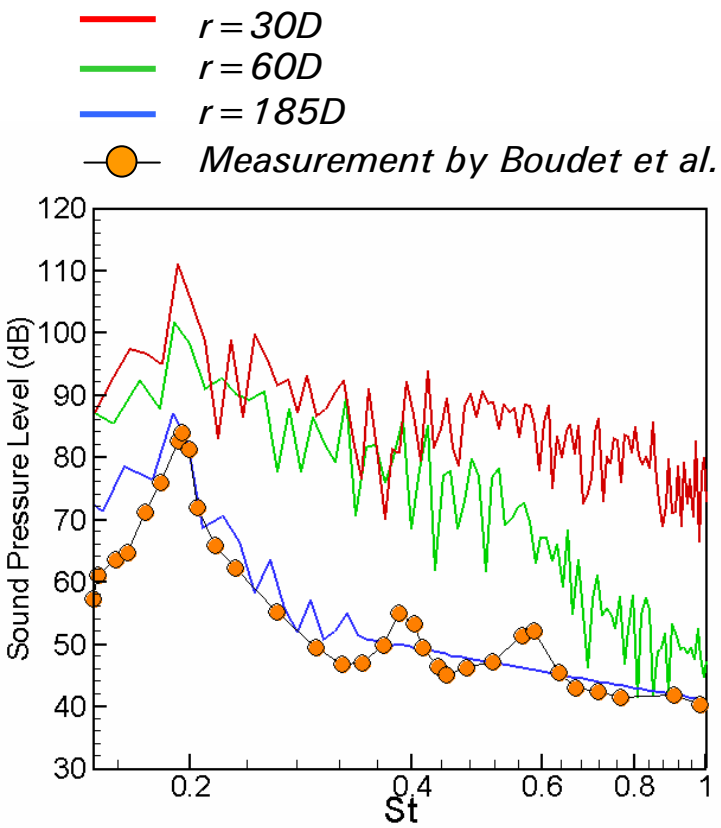

Frequency spectrum of acoustic pressure

Kato et al. (if a spanwise coherence length, $L_c \leq L_s$)

$$SPL_T = SPL_S + 10\log(L_T / L_S) \ \ (dB)$$

Validation – *iLES* (Smagorinsky model)

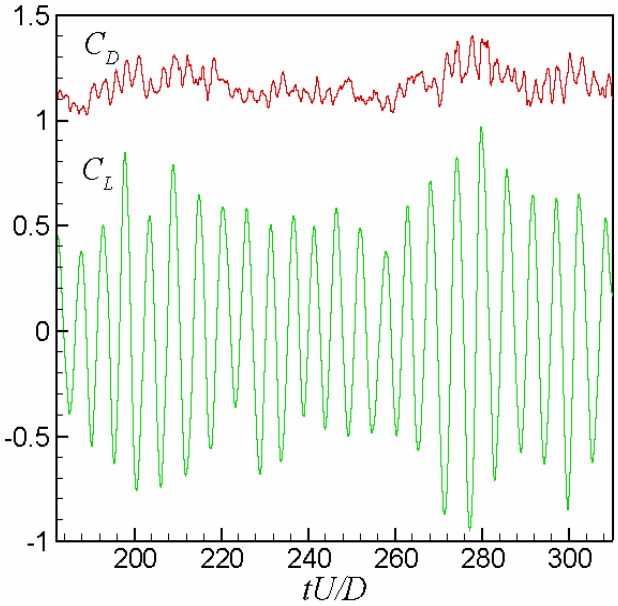

Time histories of drag and lift coefficients

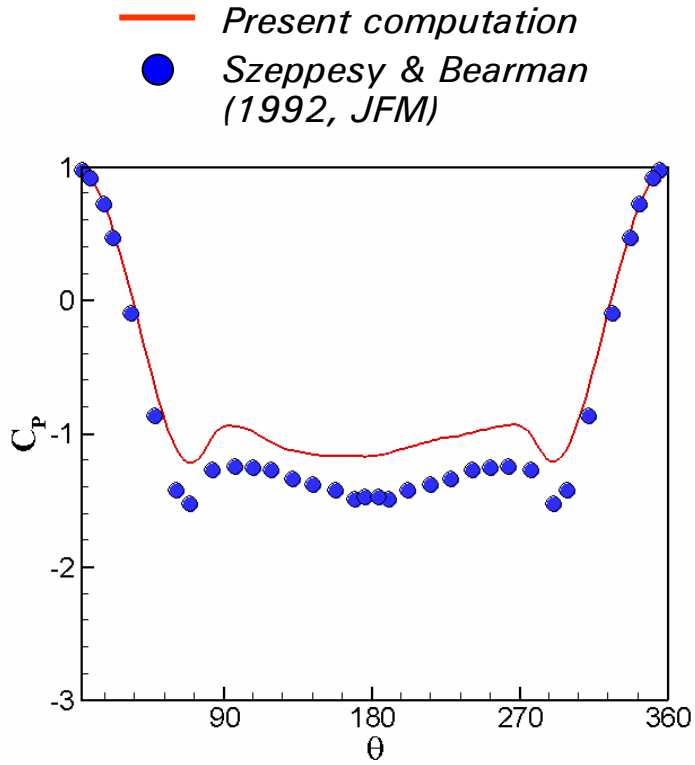

Mean pressure coefficient at the wall

Validation – *iLES* (no model)

New Calc.

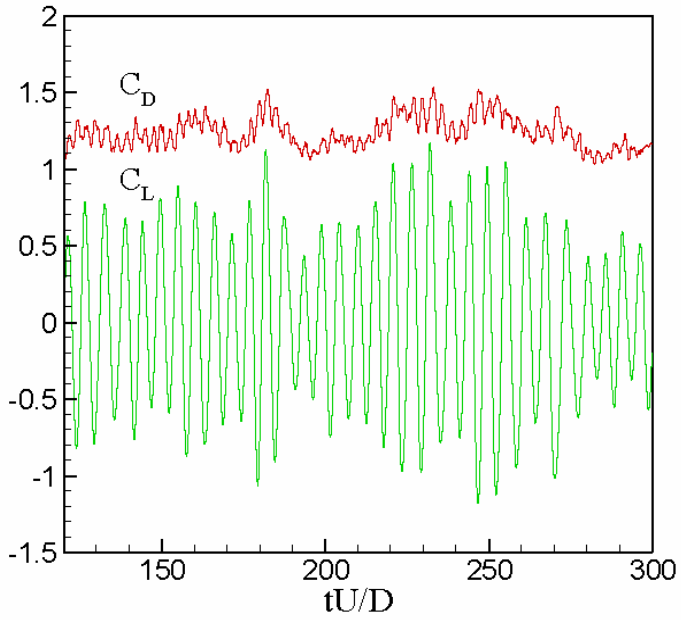

Time histories of drag and lift coefficients

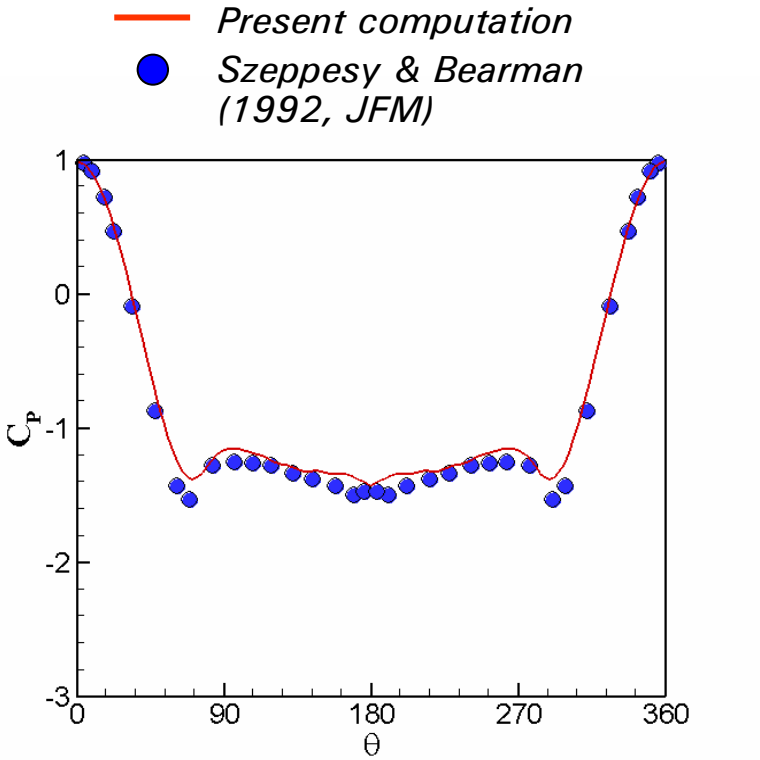

Mean pressure coefficient at the wall

Validation – Mean & Fluctuating data (no model)

New Calc.

	Present LES (*No model*)	Experiement (*Szepessy* & *Bearman*)
St	**0.19** (0.19)*	0.19
$C_{D,avg}$	**1.24** (1.15)*	1.35
$C_{D}{}'_{rms}$	**0.1** (0.067)*	0.16
$C_{L}{}'_{rms}$	**0.54** (0.44)*	0.45-0.5

Pressure fluctuation field (no model)

New Calc.

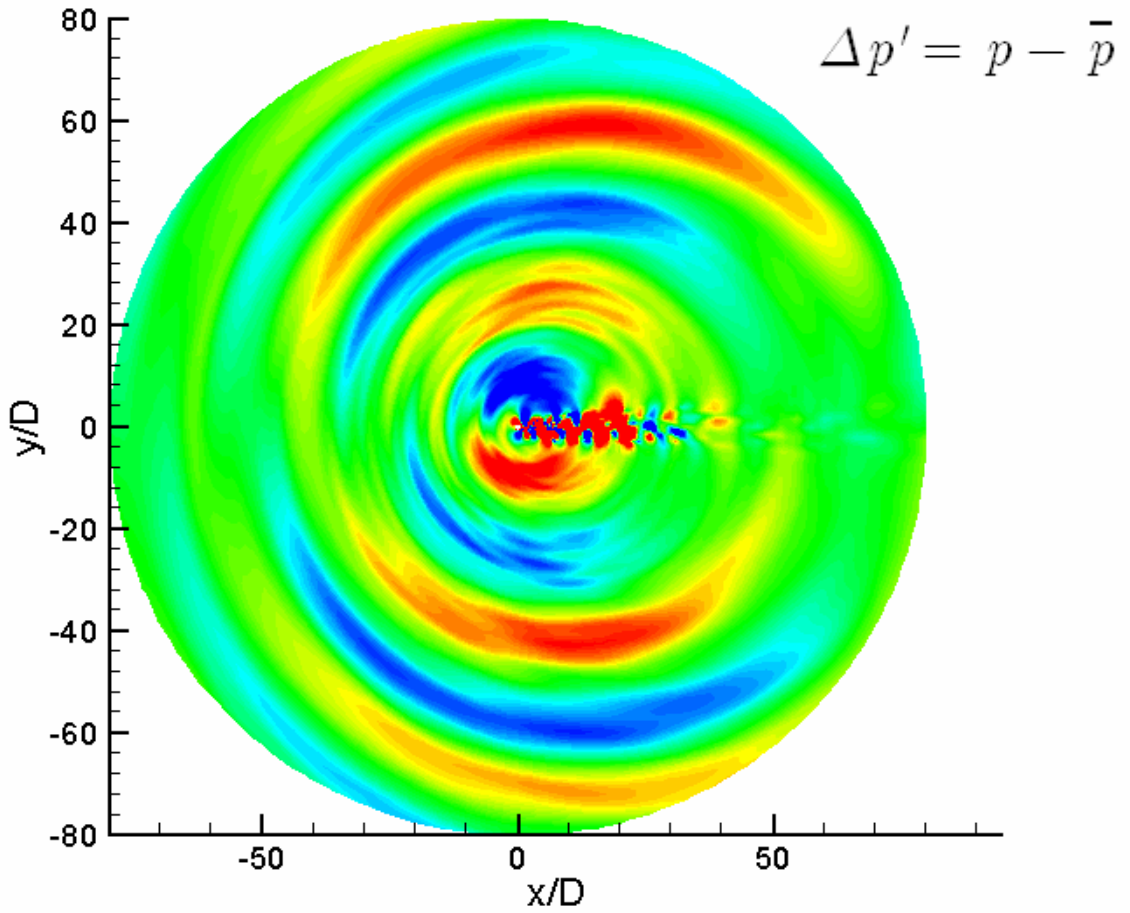

V. Phonation Aeroacoustics in Vocal Tract

Introduction

Review of Anatomy

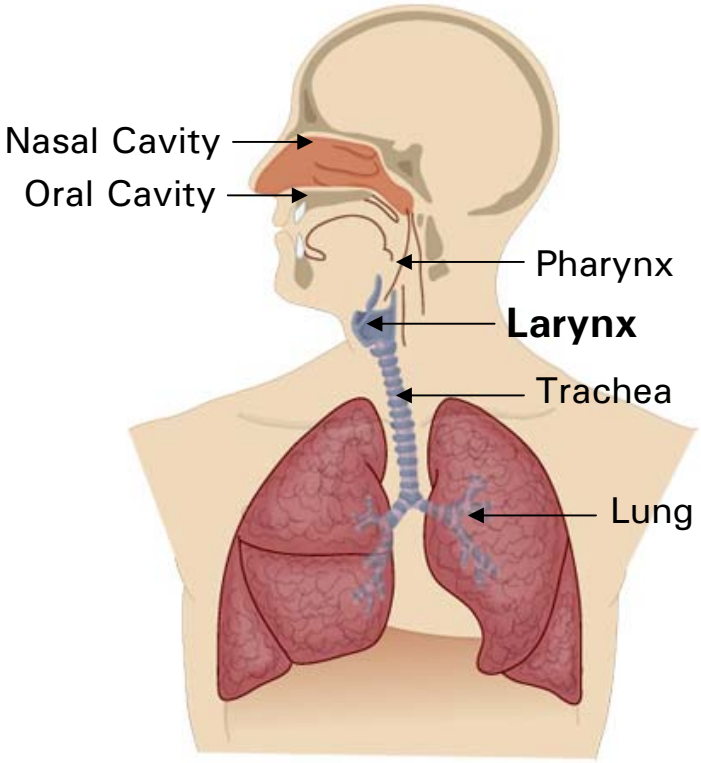

Basic components of the airway system

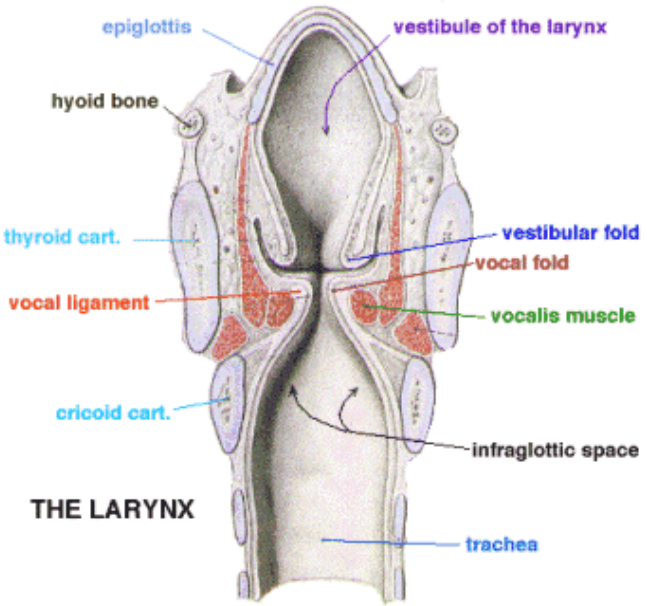

Coronal section through the larynx

Mechanism of phonation

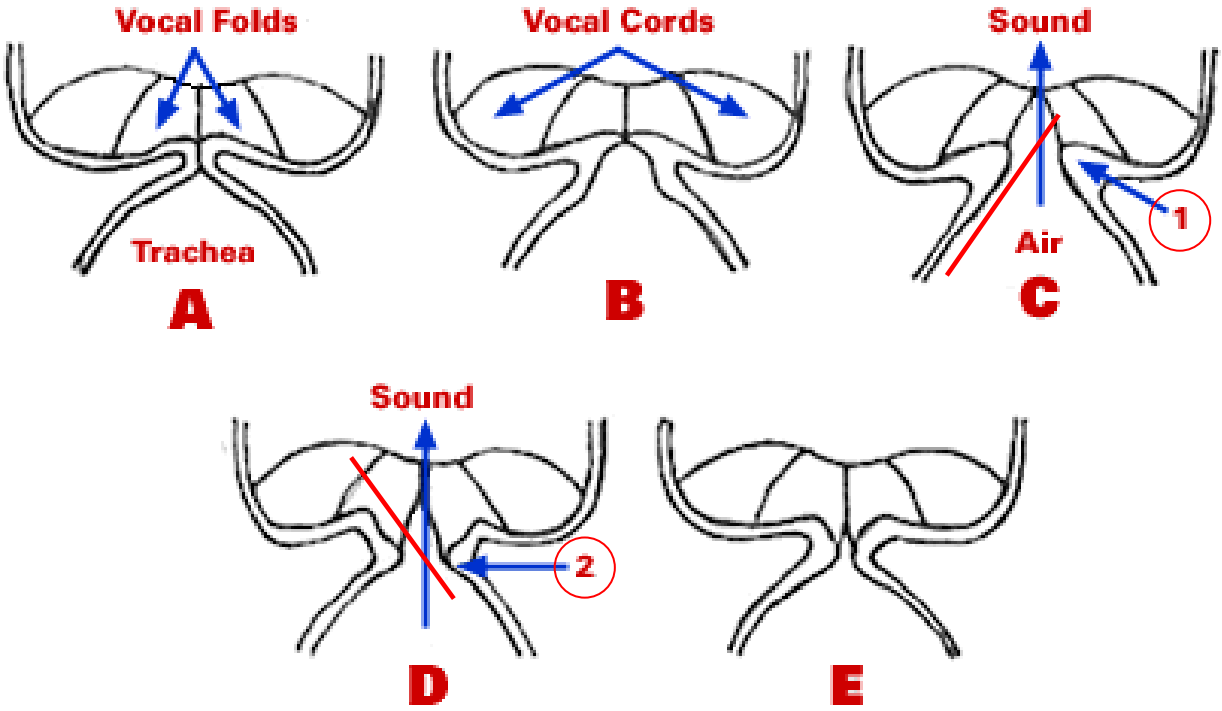

Self-sustained oscillations of the vocal folds → sound source

Computational modeling (axi-symmetric)

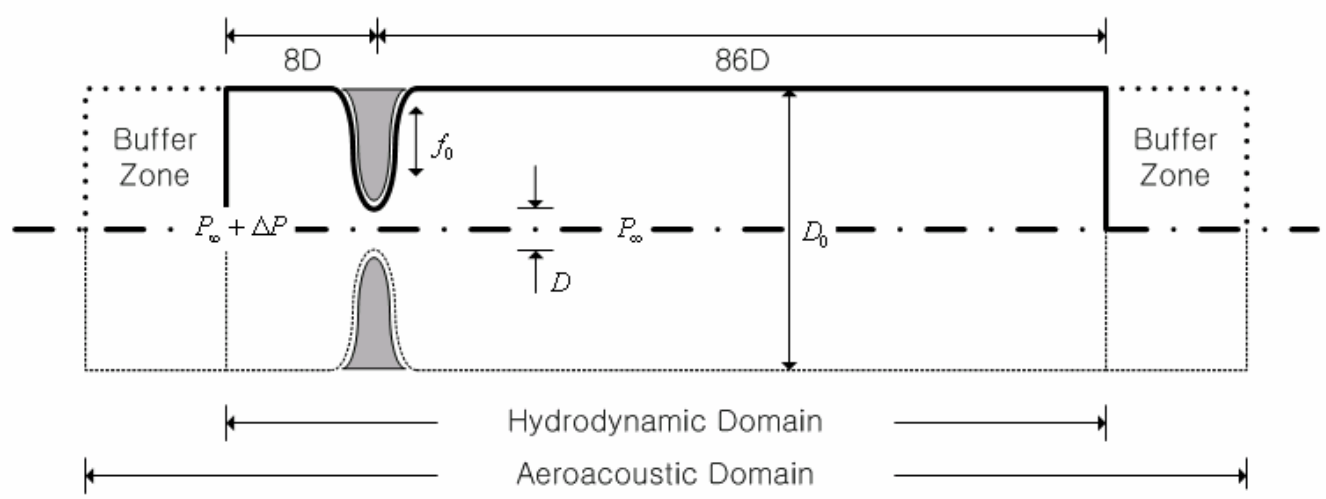

ΔP	D_{min}	D_{max}	D_0	f_0
832 Pa	0.8 mm	4.464 mm	5 D_{max}	94 Hz (*male*)

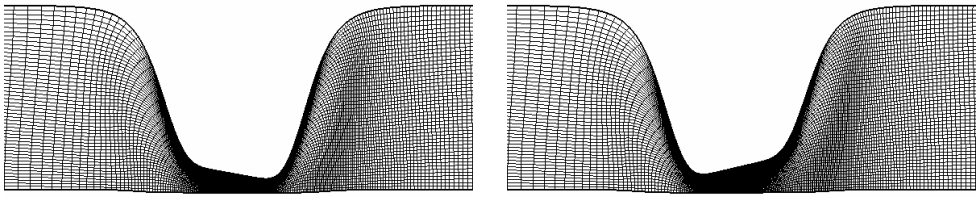

Moving hydrodynamic grid (301x51)

Governing equations

Hydrodynamic: axi-symmetric, incompressible N-S equations (***INS***) in moving coordinates,

$$\nabla \cdot \vec{U} = 0$$

$$\frac{\partial \vec{U}}{\partial t} + (\vec{U} \cdot \nabla)\vec{U} = -\frac{1}{\rho_0}\nabla P + \frac{\mu_0}{\rho_0}(\nabla^2 \vec{U})$$

Acoustic: axi-symmetric, perturbed compressible equations (***PCE***) in moving coordinates,

$$\frac{\partial \rho'}{\partial t} + (\vec{u} \cdot \nabla)\rho' + \rho(\nabla \cdot \vec{u'}) = 0$$

$$\frac{\partial \vec{u'}}{\partial t} + (\vec{u} \cdot \nabla)\vec{u'} + (\vec{u'} \cdot \nabla)\vec{U} + \frac{\rho'}{\rho}\frac{D\vec{U}}{Dt} + \frac{1}{\rho}\nabla p' = \frac{\mu_0}{\rho}(\nabla \cdot \vec{f'})$$

$$\frac{\partial p'}{\partial t} + (\vec{u} \cdot \nabla)p' + \gamma p(\nabla \cdot \vec{u'}) + (\vec{u'} \cdot \nabla)P = -\frac{DP}{Dt}$$

Glottis transient profile during motions

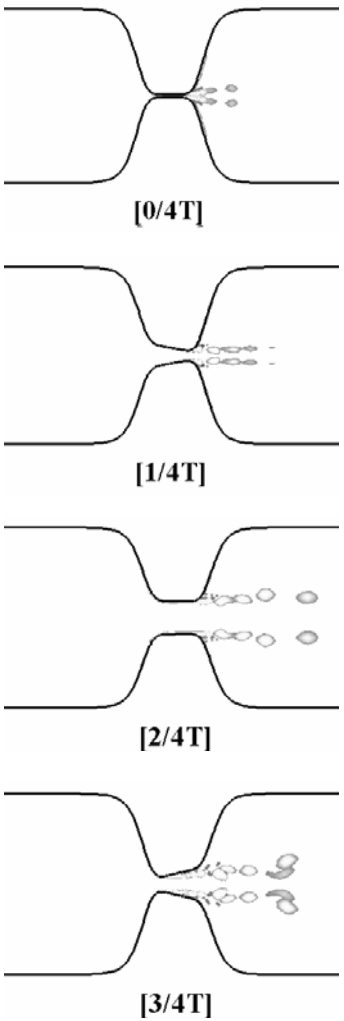

Time dependent glottal radius (Zhao et al, 2002)

$$r_w(x,t) = \frac{D_0 - D_{\min}}{4}\tanh(s) + \frac{D_0 + D_{\min}}{4} + \frac{1}{2}[1-\tanh(s)]\times[\beta_1(x+cD_{\max}) - \beta_2(x-cD_{\max})]$$

$$s = \frac{b|x|}{D_{\max}} - \frac{bD_{\max}}{|x|}, \quad \beta_2(t) = \beta_1\left(t+\frac{T}{9}\right), \quad b = 1.4 \ \textit{and} \ \ c = 0.42,$$

$$\beta_1(t) = \begin{cases} 0, & \left(t \le \frac{1}{9}T\right) \\ 0.244\left[1-\cos\left\{\frac{9\pi}{4}\left(\frac{t}{T}-\frac{1}{9}\right)\right\}\right], & \left(\frac{1}{9}T < t \le \frac{5}{9}T\right) \\ 0.488, & \left(\frac{5}{9}T < t \le \frac{6}{9}T\right) \\ 0.244\left[1+\cos\left\{3\pi\left(\frac{t}{T}-\frac{6}{9}\right)\right\}\right], & \left(\frac{6}{9}T < t \le T\right) \end{cases}$$

Moving grids for *INS* & *PCE*

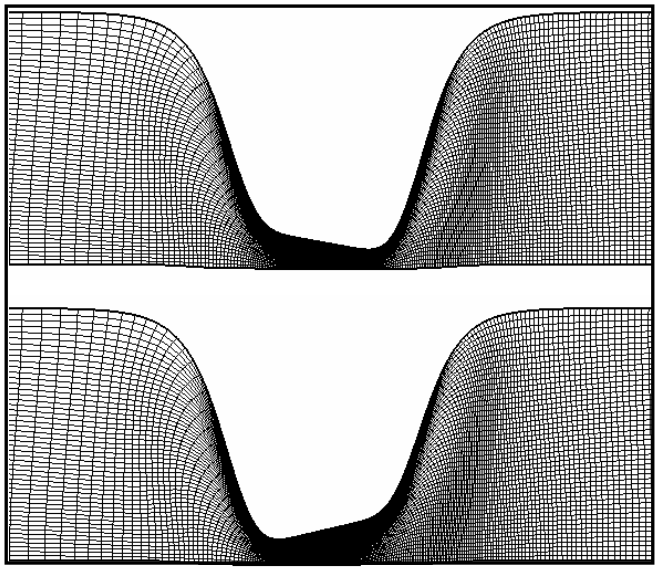

Moving **hydrodynamic** grid (301x51)

O

C

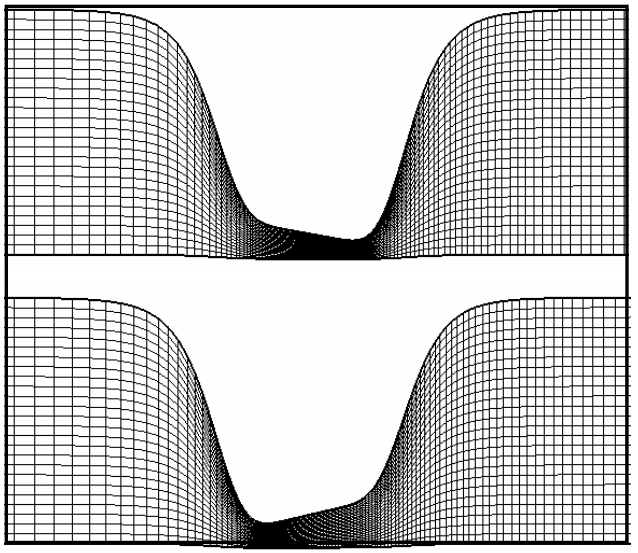

Moving **acoustic** grid (251x26)

Hydrodynamic & pressure fluctuation fields

Formation of pulsating jet (f_o) → **P(x,t) around glottis => F_x(t)**

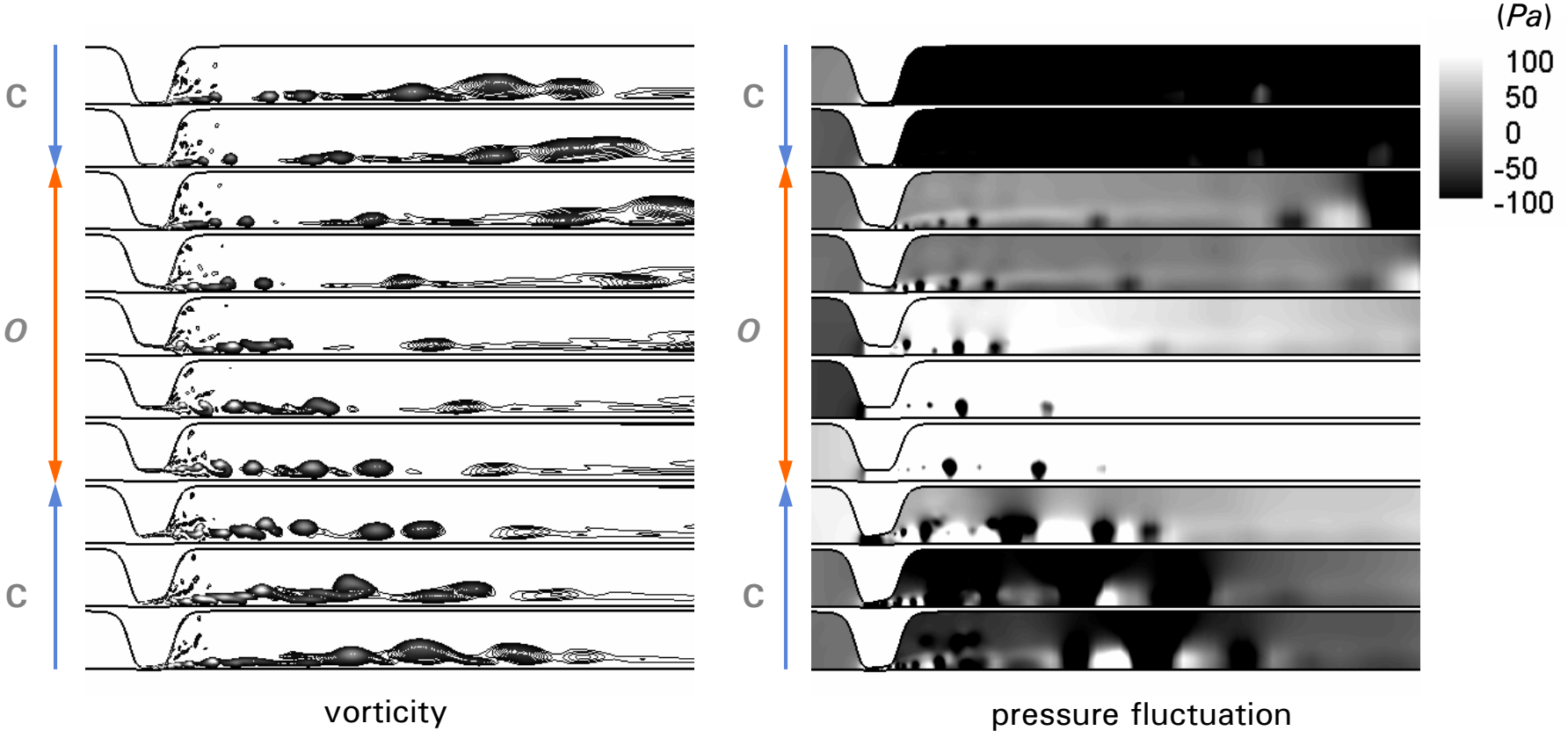

vorticity

pressure fluctuation

Among Monopole, Dipole, & Quadruple, Dipole sound dominates in vocal phonation by an (oscillating) piston effect.

1. Validation

$\Delta P = 8.1 cmH_2O, \quad f_o = 94Hz$

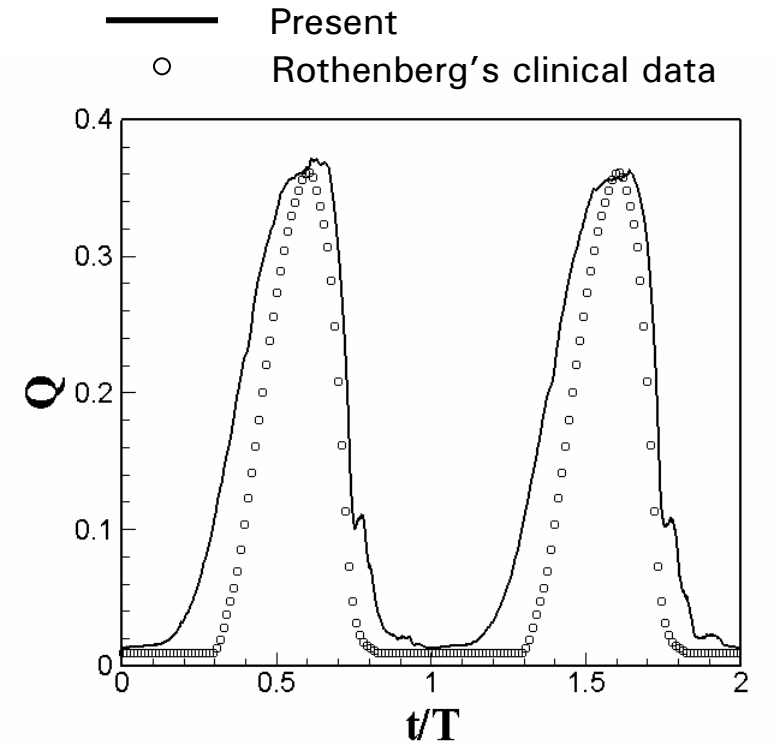

Volume flow rate (*l/s*)

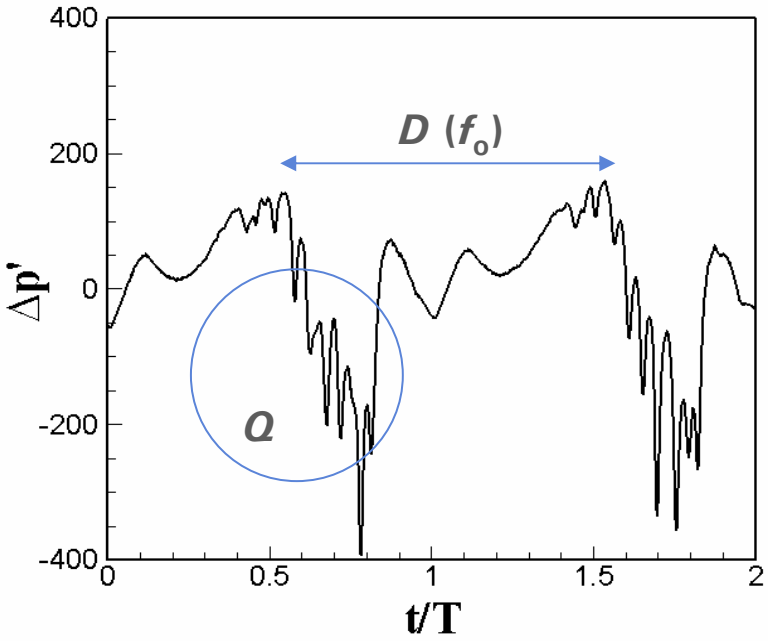

Acoustic pressure (Pa) at 10Dmax downstream

$SPL = 110dB$

2. Effect of fundamental frequency (male & female)

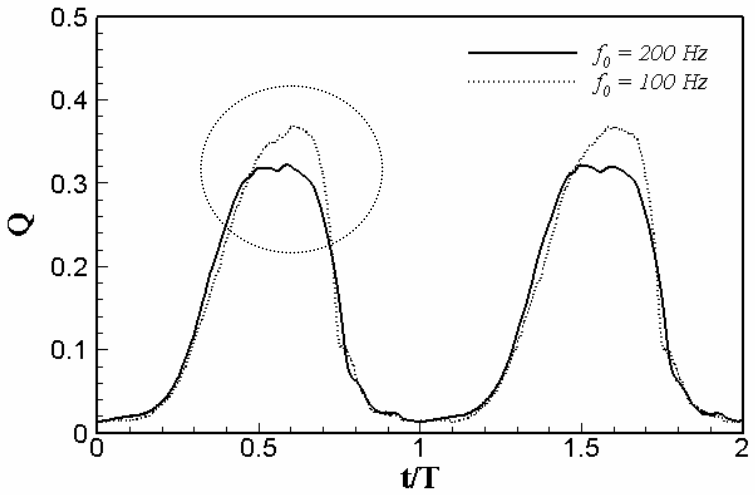

Volume flow rate (*l/s*) through the glottis

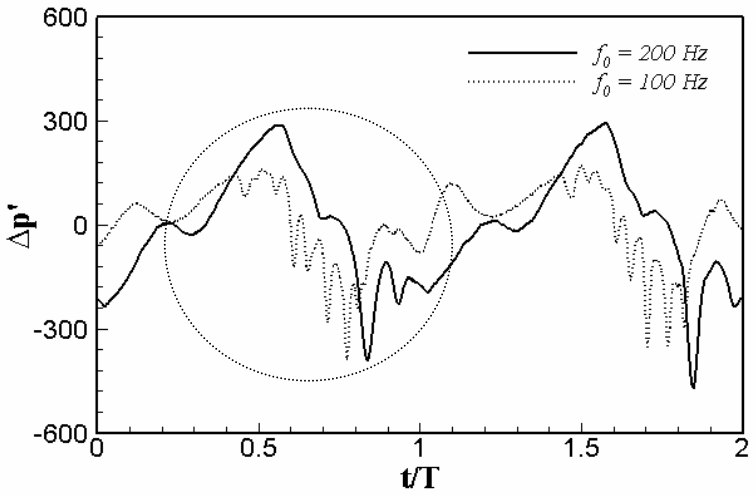

Acoustic pressure (Pa) at 10Dmax downstream

Variation of fundamental frequency → change of Jet Reynolds No.
→ change of Jet flow characteristics

High f_o generates fluty sound, while low f_o makes sound brassy

Effect of fundamental frequency (male & female)

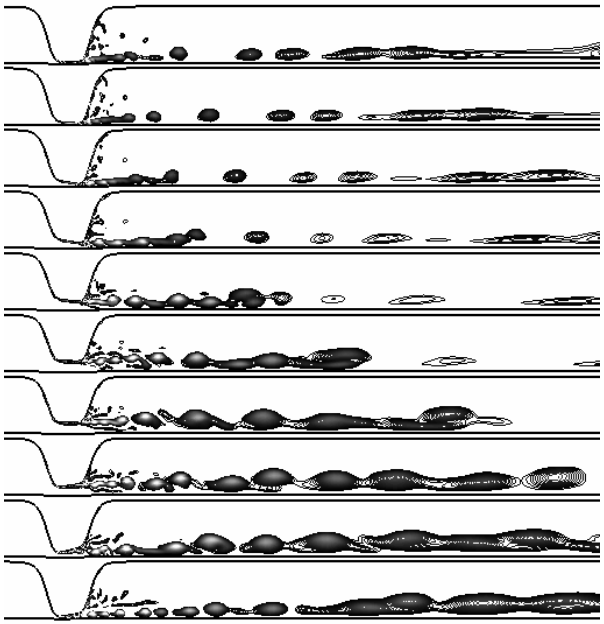

$f_0 = 94$Hz (male)

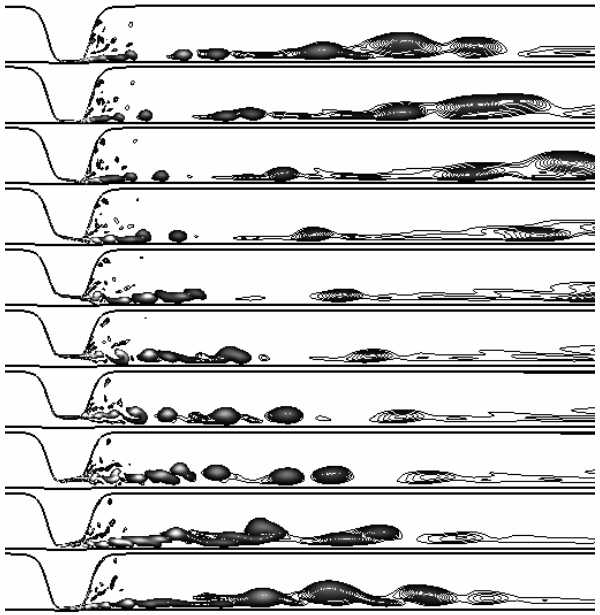

$f_0 = 200$Hz (female)

$Re_f < Re_m$

3. Effect of rotational motion of Glottis

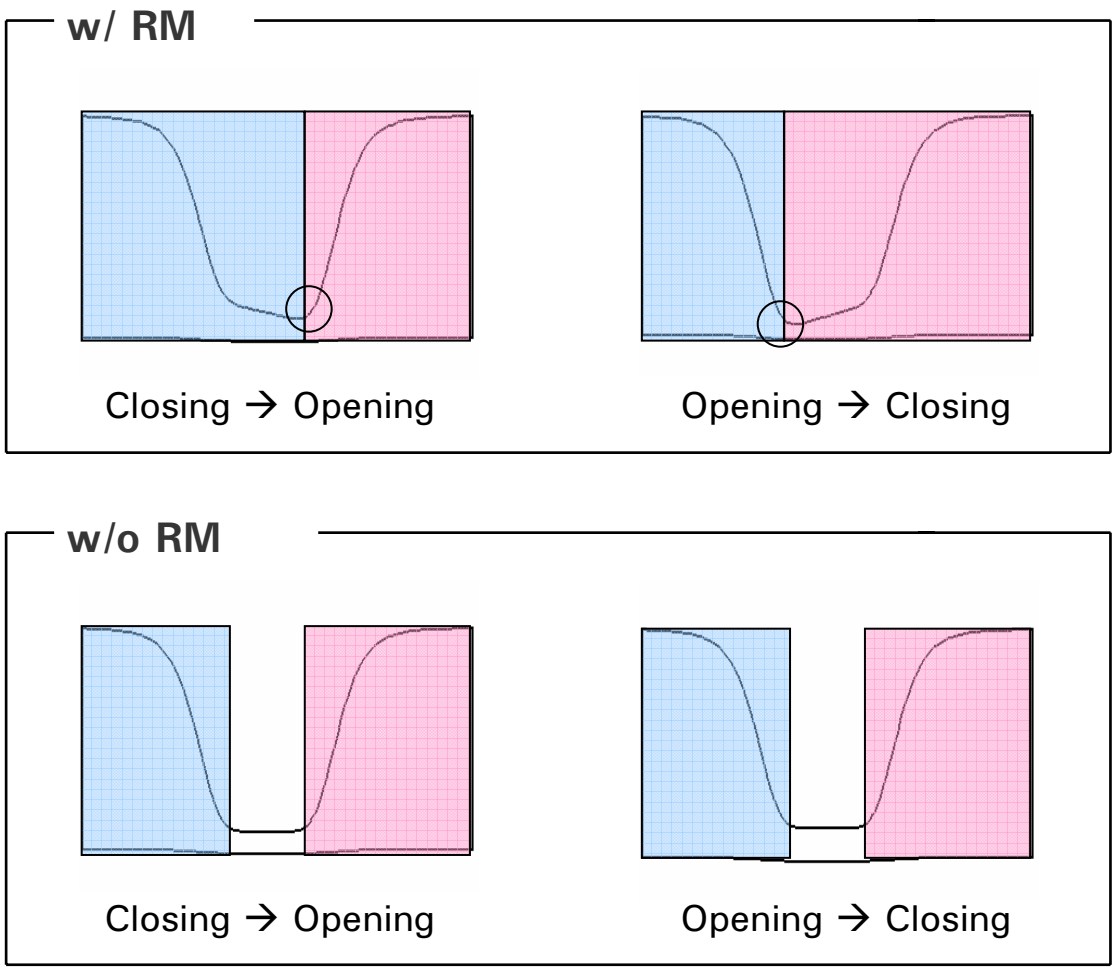

Effect of rotational motion

$f_0 = 200\text{Hz}$, $\Delta P = 8.1\text{cmH}_2\text{O}$

Glottal Resistance: $R = \Delta P/Q$ (*Van den Berg, 1957*)

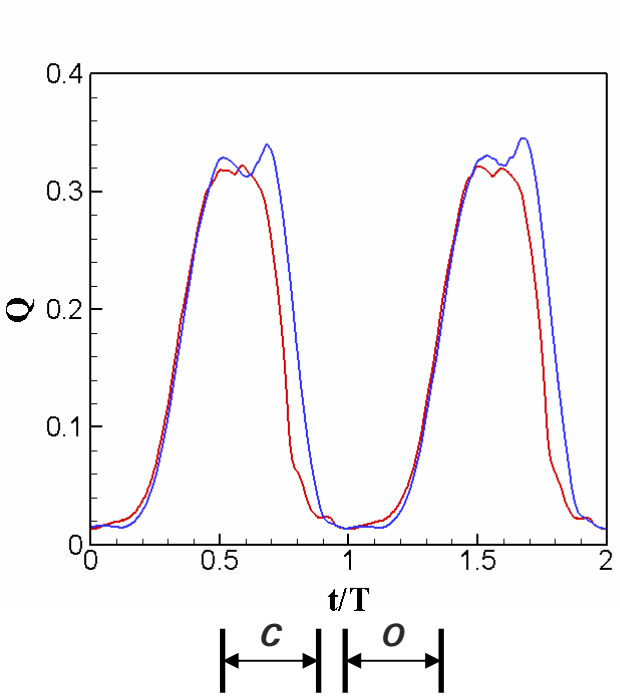

Volume flow rate (*l/s*) through the glottis

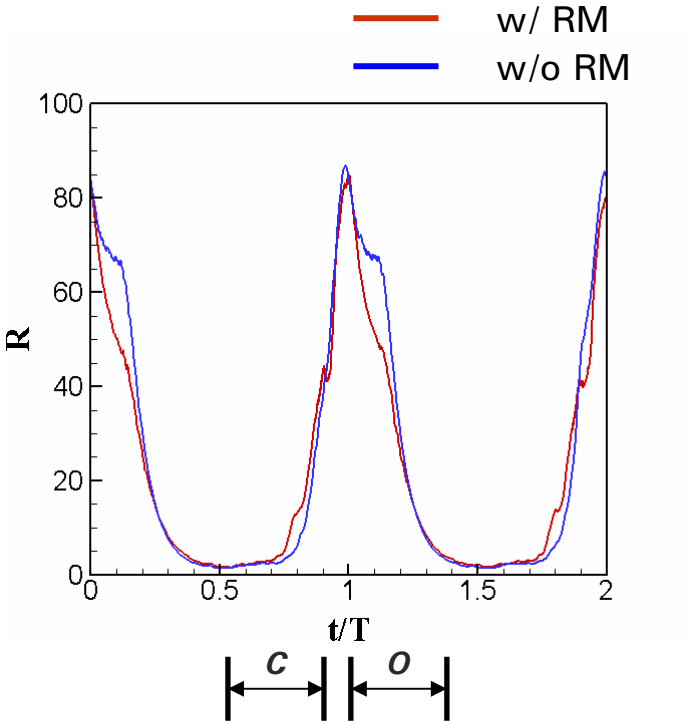

Periodic variation of glottal impedance (*kPa·s/l*)

Effects of rotational motion

For a sound generator (glottis) to be mechanically efficient, compression waves should be generated with minimum glottal resistance at opening and rarefaction waves with maximum glottal resistance at closure.

With rotational motion, *R* is clearly maximum at *C-stage* and minimum at *O-stage*, which means that *rotational motion* of glottis is related to the effectiveness of rarefaction & compression effects.

Conclusions and future work

- Understanding of sound generation mechanisms and characteristics.
- Computational results agree well with the inverse filtered data by Rothenberg.
- Fundamental frequency of glottis has effect on voice quality.
- **Rotational motion** of glottis is associated with the **efficiency** of vocal folds motion via **glottis impedance**.
- In the future, we hope to include the fluid-structure-interaction (**FSI**) to replicate the **self-sustained motions** of glottis and then the **acoustic coupling**.

Questions & Answers.

Thank you for your attentions.